

**UNIVERSIDADE FEDERAL DO ABC  
CENTRO DE CIÊNCIAS NATURAIS E HUMANAS**

**CAMILA SCHAAF BENFICA**

**A META-ANALYSIS ON GENE EXPRESSION MODULATION OF *Setaria italica* AND  
*Setaria viridis* SIBLING SPECIES IN RESPONSE TO ABIOTIC STRESS**

**SÃO BERNARDO DO CAMPO - SP**

**2023**

**CAMILA SCHAAF BENFICA**

**A META-ANALYSIS ON GENE EXPRESSION MODULATION OF *Setaria italica* AND  
*Setaria viridis* SIBLING SPECIES IN RESPONSE TO ABIOTIC STRESS**

Trabalho de Conclusão de Curso apresentado à  
Universidade Federal do ABC (UFABC), como parte  
dos requisitos para obtenção do título de Bacharela em  
Ciências Biológicas.

Orientadora: Profa. Dra. Nathalia de Setta Costa

Co-orientador: Vitor Gabriel Bucieri Theorodo

**SÃO BERNARDO DO CAMPO - SP**

**2023**

Universidade Federal do ABC

**CAMILA SCHAAF BENFICA**

**A META-ANALYSIS ON GENE EXPRESSION MODULATION OF *Setaria italica* AND  
*Setaria viridis* SIBLING SPECIES IN RESPONSE TO ABIOTIC STRESS**

Conceito: \_\_\_\_\_

**Banca Avaliadora:**

Prof.(a) Dr.(a): \_\_\_\_\_

Assinatura: \_\_\_\_\_

Prof.(a) Dr.(a): \_\_\_\_\_

Assinatura: \_\_\_\_\_

Prof.(a) Dr.(a): \_\_\_\_\_

Assinatura: \_\_\_\_\_

Data da apresentação oral: \_\_\_\_\_

Dedico este trabalho ao meu avô, Jakson Schaaf, que muito me ensinou em vida e estará sempre vivo em meu coração.

Agradeço ao meu companheiro de vida, Raidson Cerqueira, por todo o apoio que me deu durante a elaboração deste trabalho e por tudo que construímos juntos até aqui.

Aos meus pais, que me deram as melhores oportunidades e conselhos, agradeço todo o amparo, amor e carinho.

À minha orientadora, Nathalia de Setta, agradeço por toda a paciência e dedicação em ensinar, e ao meu companheiro de laboratório, Vitor Theodoro, por estar ao meu lado compartilhando as dificuldades e conquistas.

Sem vocês, este trabalho não seria possível.

“Sustainable development can be understood as the transition strategy for handling the needs of the present without compromising the well being of future generations”

**Arjan van Timmeren**

## ABSTRACT

Abiotic stressors such as water deficit, extreme temperatures and high salinity, represent significant limitations to crop yields, creating a pressing concern for global food security. With the persistent rise in temperatures and the imminent threats of climate change, the challenges facing crop production are exacerbated. *Setaria italica* and its sibling species *Setaria viridis* are emerging as Poaceae plant models due to their small diploid genome, C4 photosynthesis, short life cycle, and fully sequenced genome, these species display a natural resistance to low-water environments. To investigate the stress response in *Setaria* species, this study conducted a comprehensive meta-analysis, utilizing RNA-seq data from previous studies that explored gene expression under various abiotic stress conditions. Our findings corroborate the significant downregulation of photosynthesis during osmotic stress. Temperature and high light stress were characterized by extensive modulation of RNA biosynthesis, impacting multiple transcription factor families, as well as substantial effects on protein biosynthesis. Notably, the EIL and HSF TF families were prominent in *S. italica* during osmotic stress and *S. viridis* during temperature and high light stress, respectively. Additionally, raffinose metabolism appeared as importantly upregulated in all stress responses. An individual analysis was also conducted with the *APX* and *GPX* gene families of both species and we identified that most of the loci are modulated under abiotic stress, and that some of them are modulated into distinct co-expression networks, signifying their unique functions and independent expression. Overall, we produced a *Setaria* gene candidate catalog for further genetic studies on gene function and tolerance breeding.

**Keywords:** RNA-Seq; Poaceae; stress tolerance; APX; GPX.

## LIST OF ILLUSTRATIONS

### FIGURES

- Figure 1 - Methodology flowchart.
- Figure 2 - Venn diagram for all DEGs and most frequent DEGs in *S. italica* and *S. viridis*.
- Figure 3 - Heatmap of most frequent DEGs in *S. italica* and *S. viridis* under abiotic stress.
- Figure 4 - Mapman metabolism overview for all DEGs and DEGs present in at least 50% of the comparisons of *S. italica*.
- Figure 5 - DEG frequency ratio across BINs for all DEGs and most frequent DEGs of *S. italica*.
- Figure 6 - Photosynthesis pathway of *S. italica*.
- Figure 7- Carbohydrate metabolism *S. italica*.
- Figure 8 - Sub-BIN representation analysis of up and downregulated comparisons in the RNA biosynthesis pathway for *S. italica*.
- Figure 9 - Sub-BIN representation analysis of up and downregulated comparisons in the solute transport pathway for *S. italica*.
- Figure 10 - Mapman metabolism overview for all DEGs and DEGs present at least in 50% of the comparisons of *S. viridis*.
- Figure 11 - DEG frequency ratio across BINs for all DEGs and most frequent DEGs of *S. viridis*.
- Figure 12 - Sub-BIN representation analysis of up and downregulated comparisons in the protein biosynthesis pathway for *S. viridis*.
- Figure 13 - Carbohydrate metabolism for *S. viridis*.
- Figure 14 - Sub-BIN representation analysis of up and downregulated comparisons in the RNA biosynthesis pathway for *S. viridis*.
- Figure 15 - Sub-BIN representation analysis of up and downregulated comparisons in the solute transport pathway for *S. viridis*.



Figure 16 - Heatmaps of APX and GPX gene expression profiles (LogFC) in different tissues for *S. italica* and *S. viridis*.

Figure 17 - Gene co-expression networks (GCNs) for APX and GPX genes of *S. italica* and *S. viridis*.

## **TABLES**

Table 1 - Database information of total number of DEGs in our main dataset.

Table 2 - Papers analyzed in this study.

Table 3 - Detailed information about comparisons.

## **SUPPLEMENTARY FILES**

[Supplementary file S1](#) - Expression data

[Supplementary file S2](#) - Shared DEGs

[Supplementary file S3](#) - *Setaria italica* subBINs

[Supplementary file S4](#) - *Setaria viridis* subBINs

[Supplementary file S5](#) - Unannotated genes (BIN 35)

## LIST OF ABBREVIATIONS

APX	Ascorbate peroxidase
BINs	Gene functional category
DEGs	Differentially expressed genes
GCNs	Gene coexpression networks
GolS	Galactinol synthase
GPX	Glutathione peroxidase
LEA	Late embryogenesis abundant protein
LogFC	Expression values
PSI	Photosystem I
PSII	Photosystem II
RafS	Raffinose synthase
RNA-seq	RNA sequencing
ROS	Reactive oxygen species
TFs	Transcription factors

## SUMMARY

<b>1. INTRODUCTION.....</b>	<b>11</b>
<b>2. OBJECTIVES.....</b>	<b>14</b>
2.1. General.....	14
2.2. Specific.....	14
<b>3. MATERIALS AND METHODS.....</b>	<b>15</b>
3.1. Gene expression database assembly.....	15
3.2. Heatmaps.....	16
3.3. Functional annotation.....	16
3.4. Ascorbate and glutathione peroxidase expression under abiotic stress.....	17
<b>4. RESULTS.....</b>	<b>18</b>
4.1. Gene expression database.....	18
4.2. Functional annotation and representation analysis of <i>S. italica</i> .....	22
4.3. Functional annotation and representation analysis of <i>S. viridis</i> .....	29
4.4. Not functionally annotated genes.....	36
4.5. APX and GPX gene expression modulation in response to abiotic stress.....	36
<b>5. DISCUSSION.....</b>	<b>40</b>
5.1. Global gene expression modulation under abiotic stress.....	40
5.2. APX and GPX gene expression modulation under abiotic stress.....	46
<b>6. CONCLUSIONS.....</b>	<b>49</b>
<b>REFERENCES.....</b>	<b>50</b>
Appendix A - Articles Used In The Meta-Analysis.....	57
Appendix B - Metadata.....	59

## 1. INTRODUCTION

The prospects for climate change are concerning: global temperature will continue to increase in the near term (2021-2040) in almost all scenarios for CO<sub>2</sub> emissions, and it is very likely that the 1.5°C of maximum warming of the Paris agreement will be exceeded ([IPCC, 2022](#)). As temperatures are projected to persistently increase, the imminent consequences of climate change becomes a growing threat to food security worldwide, creating a range of challenges to crop production, including extreme temperatures and shifting precipitation patterns. Simultaneously, according to United Nations projections, by 2050 global population may reach 9.7 billion people ([UN, 2022](#)) due to which food and water demand are expected to increase up to 56% ([van Dijk et al., 2021](#)) and 30% ([Boretti et al., 2019](#)), respectively. Agriculture water use alone is projected to increase by up to 20% ([Fraiture et al., 2010](#)). Consequently, the scarcity of food supplies and limited water availability are anticipated to become major issues of concern. The alarming consequences of climate change coupled with population growth highlight the urgent need to address and mitigate the impacts on global food security. Efforts must be directed towards developing resilient agricultural systems, implementing sustainable practices, and promoting innovative technologies that can adapt to the changing climate conditions with a strong focus on efficient water management and improved crop resilience. These are key aspects for achieving crop sustainable development.

Abiotic stressors are the major factor limiting crop yield ([Garg et al., 2014](#)). These stressors include water deficit, extreme temperatures, high salinity, nutrient deficiencies, soil contamination, and various others. Different types of abiotic stressors are often intertwined and add up to each other's effects. For example, elevated temperatures result from intensified solar radiation, leading to higher light intensity, which, in turn, accelerates water evaporation, ultimately causing water deficit conditions. As a consequence, plants must employ intricate stress response networks to adapt and survive under such demanding circumstances. Several authors have already reported stagnated or decreasing yield in major C4 crops, like maize and sugarcane, in response to abiotic stress ([Supit et al., 2012](#); [Ray et al., 2012](#), [Zhao et al., 2017](#)), and efforts are being made worldwide to develop more tolerant cultivars based on conventional and molecular genetic breeding.

Plants undergo a number of changes in gene expression as a response to abiotic stress, which enables them to adapt and survive under these conditions. This reconfiguration of the plant's transcriptome in response to abiotic stress is tightly regulated and involves interconnected regulatory and metabolic pathways ([Zhang et al., 2022](#)). In order to develop effective breeding strategies for improving crop resilience it is essential to understand these patterns of gene expression modulation and their role in conferring stress tolerance. Therefore, investigating the transcriptome of tolerant plants under abiotic stress conditions can provide valuable insights into the mechanisms underlying stress responses and adaptation ([Qi et al., 2013](#), [Suguiyama et al., 2022](#)).

*Setaria italica*, known as foxtail millet, is a Poaceae species that was domesticated from its wild relative, *Setaria viridis*, more than 8,000 years ago ([Liu et al., 2016](#)). It is commonly grown in arid and semi-arid regions of China and India, showing natural resistance to low-water environments and a great water usage efficiency ([Shi et al., 2018](#); [Loni et al., 2023](#)). Due to their small diploid genome, C4 photosynthesis, short life cycle and full sequenced genome, *S. italica* and *S. viridis* are becoming novel plant models for the Poaceae family ([Doust et al., 2009](#); [Brutnell et al., 2010](#)), which includes valuable world crops like rice, maize, sorghum and wheat, being a key plant family to both human and animal food production as well as an important source of biomass to biofuel production.

C4 photosynthesis evolved from plants with C3 photosynthesis as a response to high light, high temperature and drought conditions ([Gowik et al., 2011](#)). C4 photosynthesis displays an optimized carbon concentration mechanism, reduced photorespiration and better water use efficiency when compared to C3 photosynthesis ([Pardo et al., 2021](#)). The adaptation of grass plants to harsh environments including arid and warm regions has been attributed to the evolution of C4 photosynthesis ([Osborne et al., 2009](#)). Although, this trait alone is insufficient to account for C4 plants resilience, meaning other adaptations have to be contributing to the tolerance ([Pardo et al., 2021](#)).

Exploring the mechanisms through which *Setaria* species regulate gene expression in response to abiotic stress, particularly water deficit, is of significant value in uncovering novel stress-responsive genes and pathways. Such insights can be applied in enhancing abiotic stress tolerance not only in *Setaria* but also in other major crops belonging to the same family, such as

maize and sugarcane. The genetic similarities and evolutionary relationships among these plant species increase the likelihood of shared stress-responsive mechanisms, making *Setaria* a valuable reference for discovering and implementing effective strategies in broader agricultural contexts.

RNA sequencing (RNA-seq) is a set of methodologies that provides valuable insights into the gene expression patterns, revealing which genes are being modulated to facilitate adaptation to certain environmental conditions ([Shi et al., 2018](#)). Regulation of gene expression occurs in a very complex crosstalk of biochemical pathways that result in a whole-system final response. Therefore, it is important to understand adaptation as a complex process involving multiple factors and different types of cells and tissues, rather than actions of individual genes ([Zhang et al., 2021](#)). In this study, to investigate genes involved in the stress response of *Setaria* species, a comprehensive meta-analysis was conducted using previous studies that analyzed gene expression modulation by RNA-seq of plants submitted to various types of abiotic stress. Our hypothesis is that there must be specific sets of genes in *S. italica* and *S. viridis* that are differentially expressed under abiotic stress. Whether these sets of genes exist, they might be a key component of *Setaria* species abiotic stress response and therefore can be a great target to genetic breeding. Given that abiotic stress is often a combination of multiple factors, our results can provide valuable insights for the development of molecular breeding strategies for Poaceae crops.

## 2. OBJECTIVES

### 2.1. General

- To identify pivotal genes and pathways involved in the abiotic stress response of *S. italica* and *S. viridis* sibling species.

### 2.2. Specific

- Perform a comprehensive literature search using specific databases on previously published studies that submitted *S. italica* and *S. viridis* to abiotic stress situations and had available RNA-Seq data;
- Compile RNA-seq data in a single database of relative expression values;
- Understand the broader landscape of gene expression responses under various abiotic stress conditions;
- Explore potential specificity in terms of tissue or types of stress responses within each species;
- Conduct an investigation into the functional categories that are differentially represented during the abiotic stress responses, and;
- Investigate the gene expression profiles of ascorbate and glutathione peroxidases in response to abiotic stress.

### 3. MATERIALS AND METHODS

A schematic flowchart of the methodology of this study is presented below (**Figure 1**).

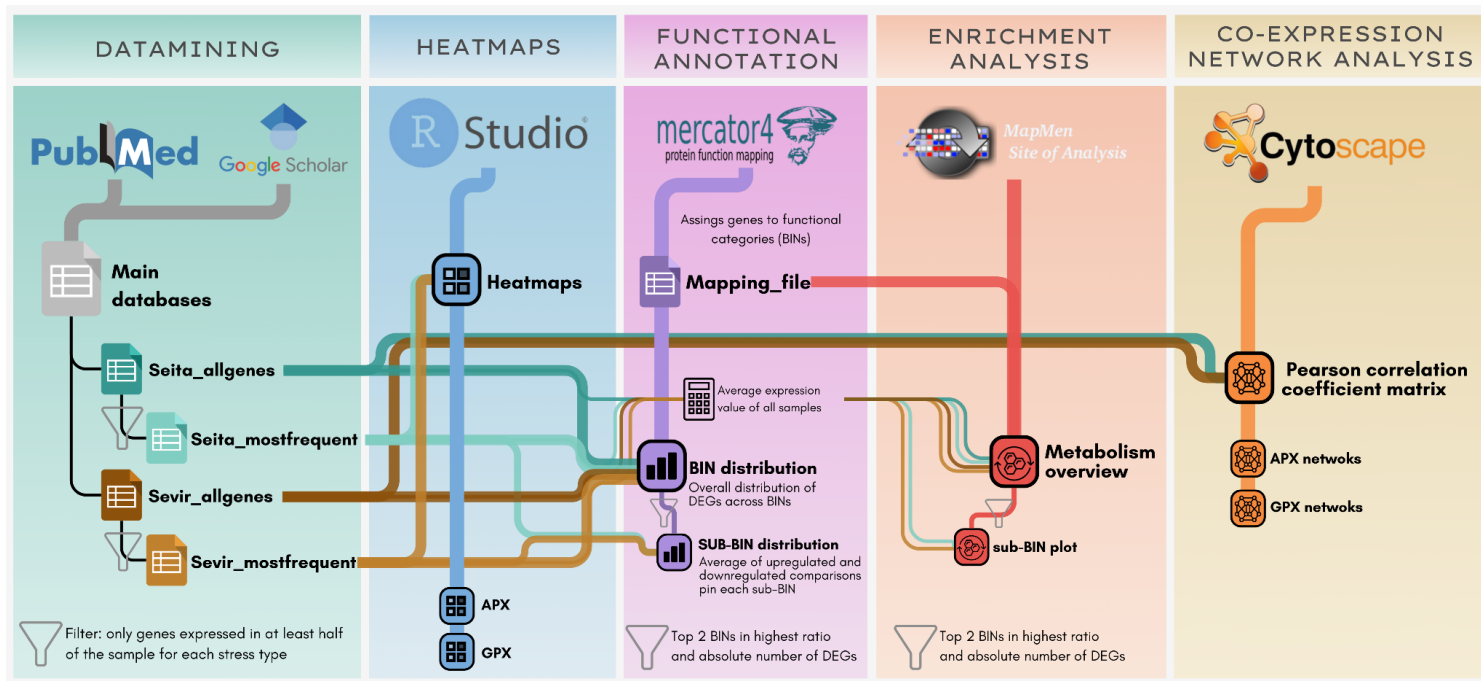


**Figure 1:** Methodology flowchart. Source: author (2023).

#### 3.1. Gene expression database assembly

A literature search was performed using the key words “abiotic stress”, “setaria”, “RNA Sequencing”, “RNA-Seq” and “transcriptome” in Google Scholar (<https://scholar.google.com/>) and PubMed (<https://pubmed.ncbi.nlm.nih.gov/>). Previously published studies of *S. italica* and *S. viridis* with available RNA-Seq data were selected and compiled in a database of relative expression values (LogFC) for each species. LogFC is a measure used to quantify the difference in expression of a gene between two experimental conditions, usually a control and a treatment sample, calculated by taking the logarithm base 10 of the ratio of expression levels between those conditions. In this way, a given LogFC value represents a comparison of how much a given gene was differentially expressed in a treatment condition compared to its control, therefore, the term “comparisons” was used in this work in reference to the values of LogFC extracted from analyzed studies. Genes were considered as differentially expressed genes (DEGs) and included



in the meta-analysis if they met the criteria of FDR-adjusted  $P \leq 0.05$  and the screening cut-off of  $\text{LogFC-ratio} \leq -1.0$  or  $\geq 1.0$ .

A metadata table was also built with biological and experimental information about samples and stress treatments retrieved from the studies, including stress type, plant tissue and growth stage. The plant growth stage was determined according to Zadoks and colleagues ([Zadoks et al., 1974](#)) using article-provided information about how old plants were when RNA was extracted for RNA-seq analysis and morphological information.

### **3.2. Heatmaps**

Heatmaps are graphical representations of data that display false color images representing values in a visual color scale. They are particularly valuable in clustering large datasets by their similarity and are often used to display RNA-seq data. In this study, we used the R package pheatmap 1.0.12 ([Kolde et al., 2019](#)) and RStudio version 4.3.1 ([R Core Team, 2023](#)) to generate heatmaps, utilizing the euclidean method for clustering of both columns and rows. For the distance calculation, we applied the ward D method ([Murtagh et al., 2014](#)). To improve clustering identification of the heatmaps, we enriched them with annotations about stress types and plant tissues.

### **3.3. Functional annotation**

Protein sequences and gene annotation tables of *S. viridis* genome v1.1 and *S. italica* genome v2.2 were extracted from the Phytozome database ([Goodstein et al., 2012](#)). Functional annotation was performed using Mercator v5.0 ([Lohse et al., 2013](#)). Mercator performs hierarchical functional annotations to protein sequences dividing them in functional categories known as BINs, which are further divided into sub-BINs. It is worth noting that each gene can belong to more than one BIN. Mercator results serve as a mapping tool in the subsequent pathway analysis using Mapman software ([Thimm et al., 2004](#)). We plotted Mapman pathways using the mean  $\text{LogFC}$  of each DEG, because Mapman can only plot pathways of one experiment at a time, meaning each gene can be linked to only  $\text{LogFC}$  value. While the averaged pathway analysis is useful for identifying the major trends and DEG-enriched pathways in the

dataset, it is essential to keep in mind that gene expression variations might not be fully captured in this approach.

Using Microsoft Excel, the results from the functional annotations were plotted in graphs. To avoid potential biases related to the number of genes in each BIN, we calculated the DEG frequency ratio by dividing the total number of DEGs in each BIN by the total number of genes within that specific BIN. This process helps to account for any variations in BIN size among the functional categories. To better understand gene expression modulation profiles, we performed a more detailed analysis that focused on sub-BIN information. For this analysis, hereafter called sub-BIN representation analysis, we calculated a ratio of the number of upregulated or downregulated comparisons, i.e. the number of LogFC values, divided by the number of DEGs in each sub-BIN.

### **3.4. Ascorbate and glutathione peroxidase expression under abiotic stress**

A detailed analysis of the ascorbate peroxidase (*APX*) and glutathione peroxidase (*GPX*) gene families was conducted in this study using our gene expression database. The annotation of *APX* and *GPX* genes from *S. italica* and *S. viridis* genomes was performed in collaboration with the master's student Vitor Gabriel Bucieri Theorodo from the Graduate Program in Biotecnociência (UFABC). To visualize the expression values of *APX* and *GPX* genes, heatmaps were generated using Microsoft Excel's conditional formatting tool.

Additionally, we constructed Gene Coexpression Networks (GCNs) using the Expression Correlation Networks tool (<https://apps.cytoscape.org/apps/expressioncorrelation>) as implemented in the Cytoscape platform ([Shannon et al., 2003](#)). Expression Correlation Networks tool calculates matrices of Pearson Correlation Coefficient similarities ( $\rho$ ) using expression values from large datasets. Then, similarity values were used to construct directed forced organic networks using Cytoscape. In the GCNs, nodes represent genes, and edges represent similarity between vectors of the expression levels across comparisons ([Buti et al., 2019](#)). Similarity values were considered significant if they met the criteria of screening cut-off of  $\rho \leq -0.8$  or  $\rho \geq 0.8$ .

## 4. RESULTS

### 4.1. Gene expression database

A total of 13 previously published studies with available RNA-seq data (**Appendix A**) of *S. italica* and *S. viridis* were selected and had their LogFC values compiled ([S1 - Expression data](#)), as well as data about stress type, tissue and stage of development of the plants (**Appendix B**). The dataset consisted of 37 distinct comparisons involving *S. italica* (**Table 1**). Among them, 10 comparisons were related to salt stress: four from seed tissue, four from root tissue, and two from shoot tissue. There were 25 comparisons tied to drought stress: 19 from shoot tissue and six from root tissue. Two comparisons were associated with PEG-induced drought stress: one from seed tissue and one from shoot tissue. For *S. viridis*, there were a total of 12 comparisons that covered different stress conditions: three each from heat stress and high light stress and six from cold stress, all of which were extracted from shoots tissue.

**Table 1.** Database information of total number of DEGs in our main dataset.

Species	All DEGs	Most frequent DEGs	Comparisons
<i>Setaria italica</i>	22,655	3,457	37
<i>Setaria viridis</i>	7,990	3,853	12

Source: Author (2023)

Across these comparisons, a substantial number of DEGs were identified: a total of 22,655 and 7,990 DEGs were found in *S. italica* and *S. viridis*, respectively (**Table 1**). Specifically focusing on drought stress comparisons, a total of 20,867 genes exhibited modulation, whereas salt stress modulated 14,572 genes, and PEG-induced stress 3,014 genes. A convergence of 10,300 DEGs was observed between salt and drought stress and 410 DEGs were shared between PEG and drought stress, constituting a remarkable 97% overlap of genes present in PEG-induced stress with the other types of stress (**Figure 2A**). Furthermore, an intersection of 2,525 DEGs emerged from all three stress types ([S2 - Shared DEGs](#)). For *S. viridis*, cold stress modulated 6,112 genes, followed by high light and heat stress with 3,187 and 1,644 genes, respectively ([S2 - Shared DEGs](#)). In terms of overlaps, 1,451 DEGs were shared between high light and cold stress, 353 DEGs were common between heat and cold stress and 268 DEGs were

common between heat and high light stress and (**Figure 2B**). All three stress types converged on 441 shared DEGs ([S2 - Shared DEGs](#)).

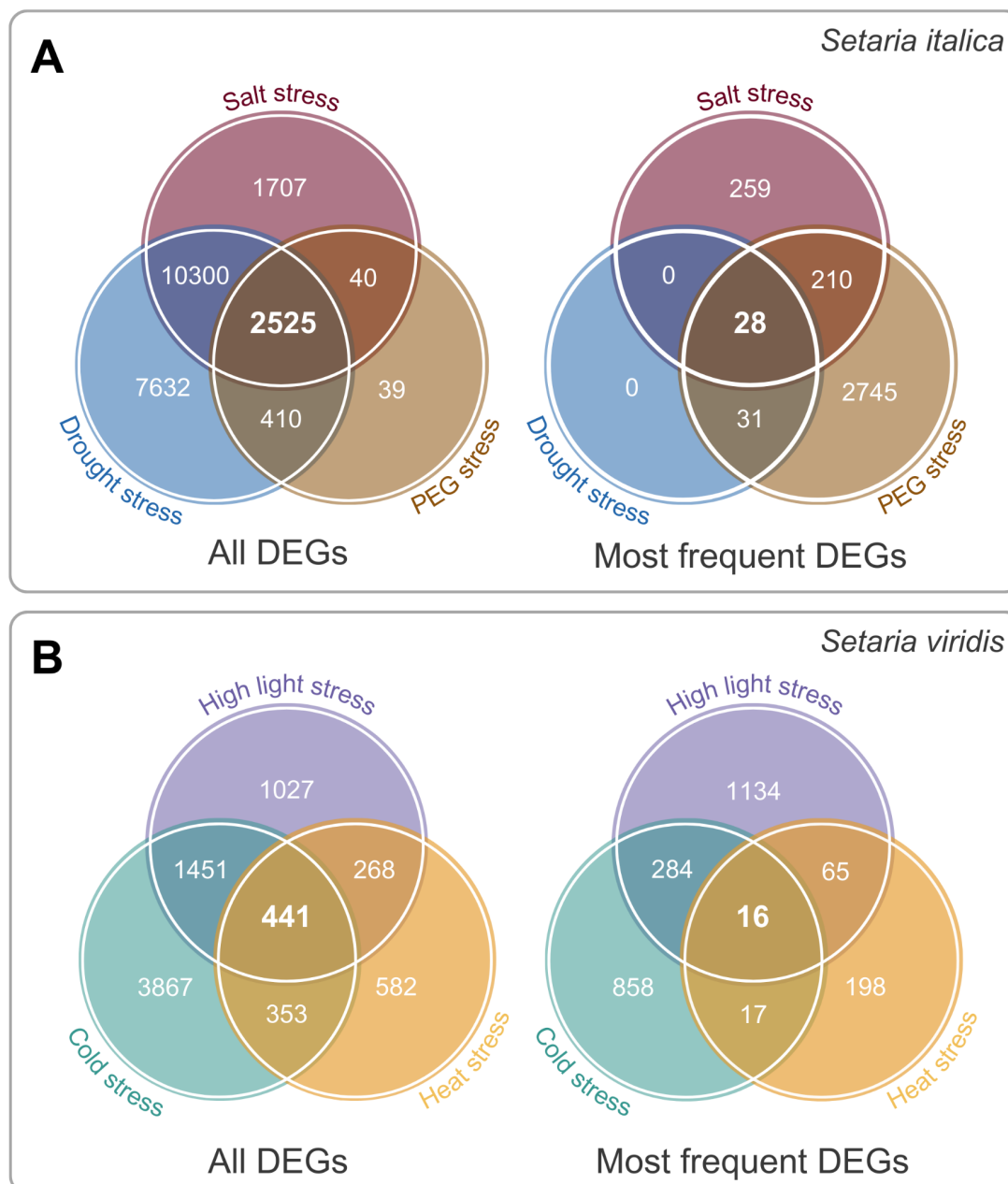
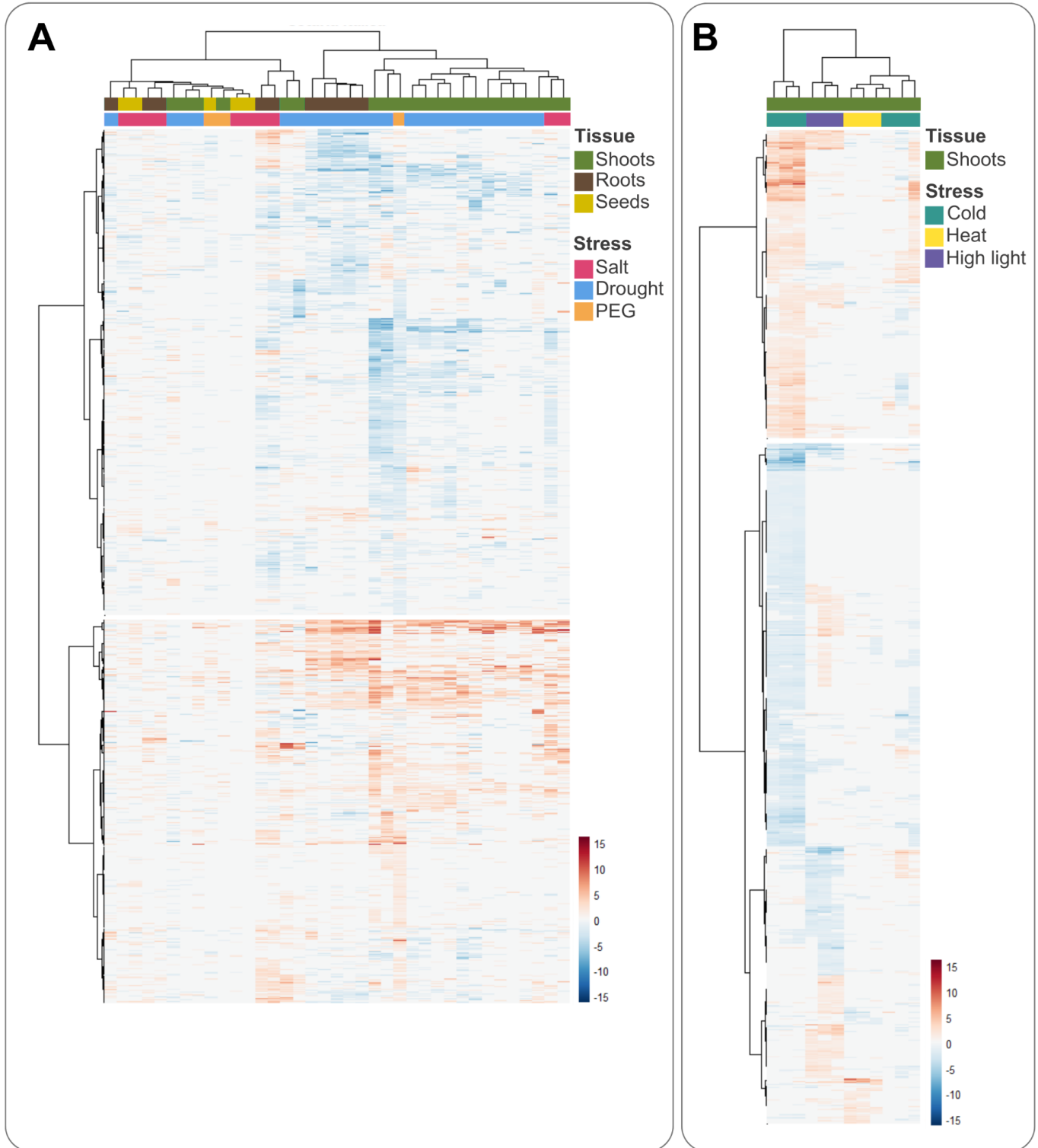


**Figure 2.** Venn diagrams for all DEGs and most frequent DEGs in *S. italica* (A) and *S. viridis* (B).

To focus on the most consistent set of DEGs, the dataset was further filtered to include only those genes expressed in at least half of the comparisons, hereafter also called as most frequent DEGs. Following this filtering step, 3,457 DEGs in *S. italica* and 3,853 DEGs in *S.*

*viridis* were retrieved (**Table 1**). Specifically, PEG-induced stress modulated 3,014 genes, while salt stress modulated 497 genes and drought stress 59 genes ([S2 - Shared DEGs](#)). Thirty-one genes modulated on drought stress were also modulated in PEG stress, and PEG and salt stresses shared 210 genes (**Figure 2A**). Additionally, 28 DEGs were shared between all stresses for *S. italica*. For *S. viridis*, high light stress modulated 1,499 genes, cold stress modulated 1,175 and heat stress 296. High light stress shared 284 and 65 DEGs with cold and heat stress, respectively. Heat and cold stress modulated 17 DEGs in common (**Figure 2B**). Sixteen DEGs were shared between all three stresses.

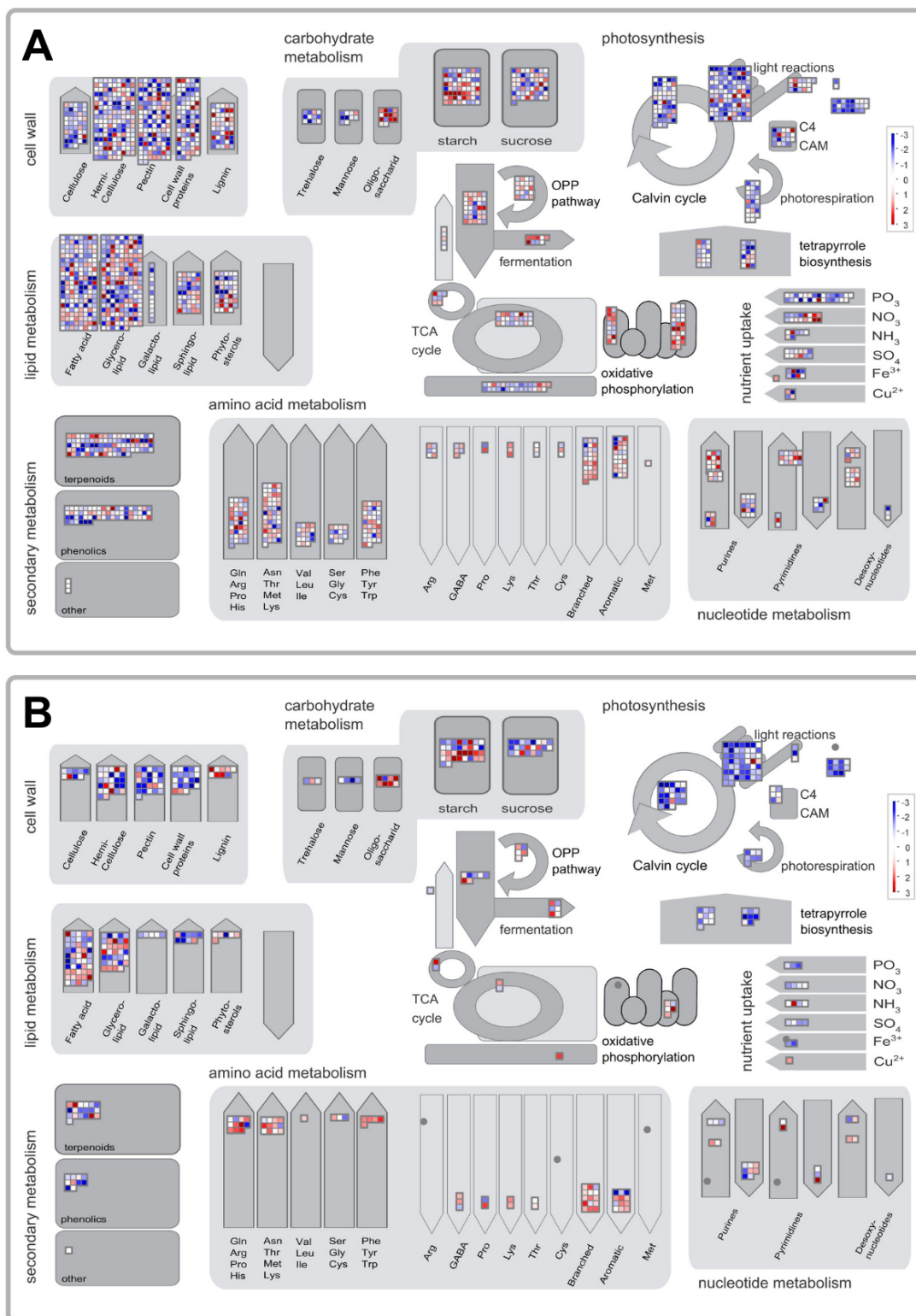
The clustered heatmaps provided insights into the overall expression patterns of the genes under different stress conditions and tissues. In the case of *S. italica*, the heatmap analysis revealed two distinct clusters of predominantly up or downregulated DEGs (**Figure 3A**). As for DEGs, the dendrogram of comparisons is divided into primary clusters, each further branching into two distinct sub-clusters. The division of clusters does not follow stress types, yet the upper right cluster displays a partition between root and shoot tissues that appear to reveal a different set of the downregulated genes. On the other hand, the left cluster does not differentiate between tissue types or stress conditions. However, all comparisons involving seed tissue reside within this cluster, which is also characterized by a visibly lower count of genes with significant LogFC values. In *S. viridis*, we also identified two clusters separating down and upregulated genes, as well as the distinct stress types, with exception of cold stress comparisons that were divided in two clusters (**Figure 3B**). Cold stress exhibited differential expression in more genes than other analyzed stresses. It was also noted that cold stress modulates a different set of genes than heat stress and only a modest degree of genes overlap with those influenced by high light stress, showing a clear distinction on the bottom cluster. Moreover, the bottom cluster unveils genes with heightened expression levels primarily under high light stress.



**Figure 3.** Heatmap of most frequent DEGs in *S. italica* (A) and *S. viridis* (B) under abiotic stress. Tree on the left of the heatmaps indicates clusters of genes and the upper tree indicates clusters of comparisons.

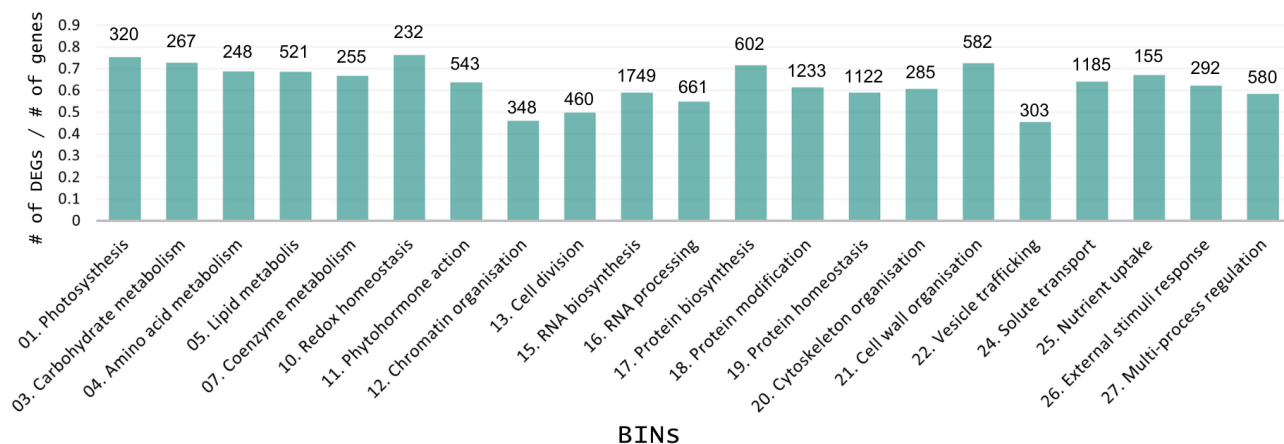
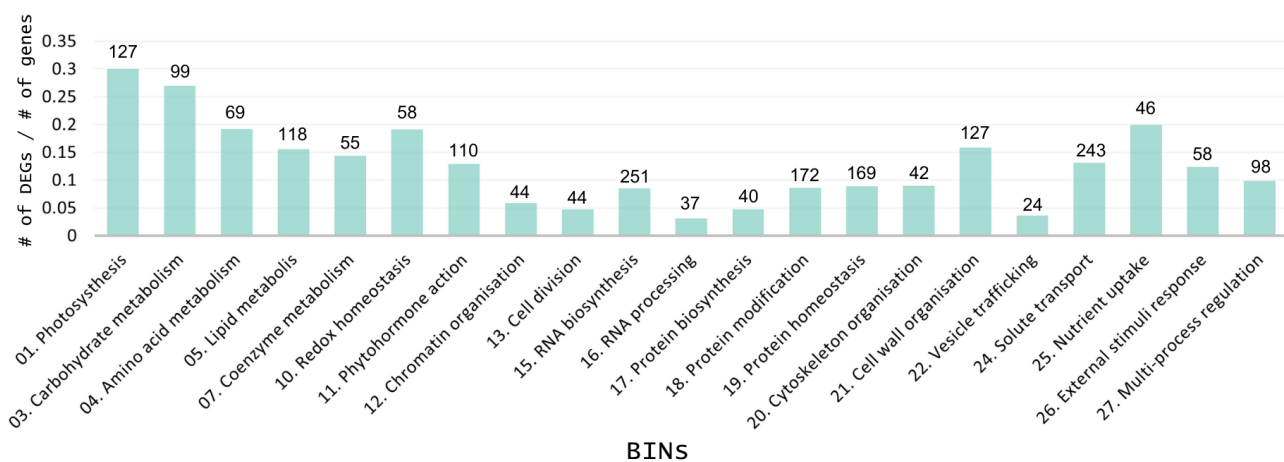
#### 4.2. Functional annotation and representation analysis of *S. italica*

Mapman and Mercator tools were utilized to functionally annotate and visualize DEGs across various regulatory and metabolic pathways. The Mapman metabolism overview for all DEGs of *S. italica* revealed gene modulation in various processes and pathways (**Figure 4A**), this pattern remained consistent even when focusing on DEGs expressed at least in 50% of the comparisons (**Figure 4B**). For most frequent DEGs, photosynthesis stood out by having almost entirely downregulated genes. The DEG frequency ratio for all DEGs revealed the highest ratios for redox homeostasis (BIN 10), followed by photosynthesis (BIN 01) and carbohydrate metabolism (BIN 03, **Figure 5A**). However, photosynthesis and carbohydrate metabolisms exhibit the highest DEG frequency ratios among the most frequent DEGs (**Figure 5B**). In terms of absolute number of DEGs, RNA biosynthesis (BIN 15) and protein modification (BIN 18) emerged as the top bins for all DEGs (**Figure 5A**); and RNA biosynthesis and solute transport (BIN 24) emerged as the most important BINs when accounting for the most frequent DEGs (**Figure 5B**).



**Figure 4.** Mapman metabolism overview for all DEGs (A) and DEGs present in at least 50% of the comparisons (B) of *S. italica*, respectively



*Setaria italica***A****All DEGs****B****Most frequent DEGs**

**Figure 5.** DEG frequency ratio across BINS for all DEGs (A) and most frequent DEGs (B) of *S. italica*, respectively. The absolute numbers of DEGs are shown above bars. Only BINS with at least 1% of the mapped DEGs were shown.

Given the prominence of the photosynthesis pathway (BIN 1) in both metabolism overview plot and DEG frequency ratio analysis, an in-depth examination was conducted. The examination encompassed the averaged plot of photosynthesis pathway from Mapman and the sub-BIN representation analysis, which was calculated by dividing the number of up or downregulated comparisons by the number of DEGs in each sub-BIN. When analyzing the photosynthesis pathway in the Mapman plot, we confirmed downregulation in almost all mapped components (**Figure 6A**). Additionally, the sub-BIN representation analysis confirmed that the majority of DEGs related to photosynthesis were downregulated throughout our comparisons, with sub-BINs being predominantly downregulated in photophosphorylation (BIN 1.1), Calvin cycle (BIN 1.2) and photorespiration (BIN 1.3, **Figure 6B**). However, transketolase (BIN 1.2.7) and phosphoenolpyruvate carboxylase activity (BIN 1.4.2) showed upregulation. Transketolase was the most represented sub-BIN, with related genes being differentially expressed on average in 17 out of 37 comparisons ([S3 - Seita sub-BINs](#)).

The second most representative functional category was carbohydrate metabolism. The Mapman plot for most frequent DEGs showed modulation of starch and sucrose metabolisms (**Figure 7A**). The sub-BIN representation analysis revealed that oligosaccharide metabolism (BIN 3.4) not only stood out but also presented the sub-BINs with the highest level of upregulation and representation across the comparisons, which were galactinol synthase (GolS, BIN 3.4.1) and raffinose synthase (RafS, BIN 3.4.3, **Figure 7B**). Sub-BIN representation analysis was also performed in the two functional categories with higher absolute number of DEGs in the DEG frequency ratio analysis (**Figure 5A and B**). For RNA biosynthesis (BIN 15), it is possible to note that transcriptional regulation (BIN 15.5) was most represented (**Figure 8**), with specifically 237 DEGs that belong to several subfamilies of transcription factors (TFs) being modulated ([S3 - Seita sub-BINs](#)). Finally, the solute transport category (BIN 24) had the carrier-mediated transport BIN (BIN 24.2) as the sub-BIN with most DEGs (n = 188, [S3 - Seita sub-BINs](#)), although mechanosensitive ion channel (MLS, BIN 24.3.5) was the most frequent thorough comparisons (24.3.5, **Figure 9**). Interestingly, it was found to be upregulated in all comparisons.

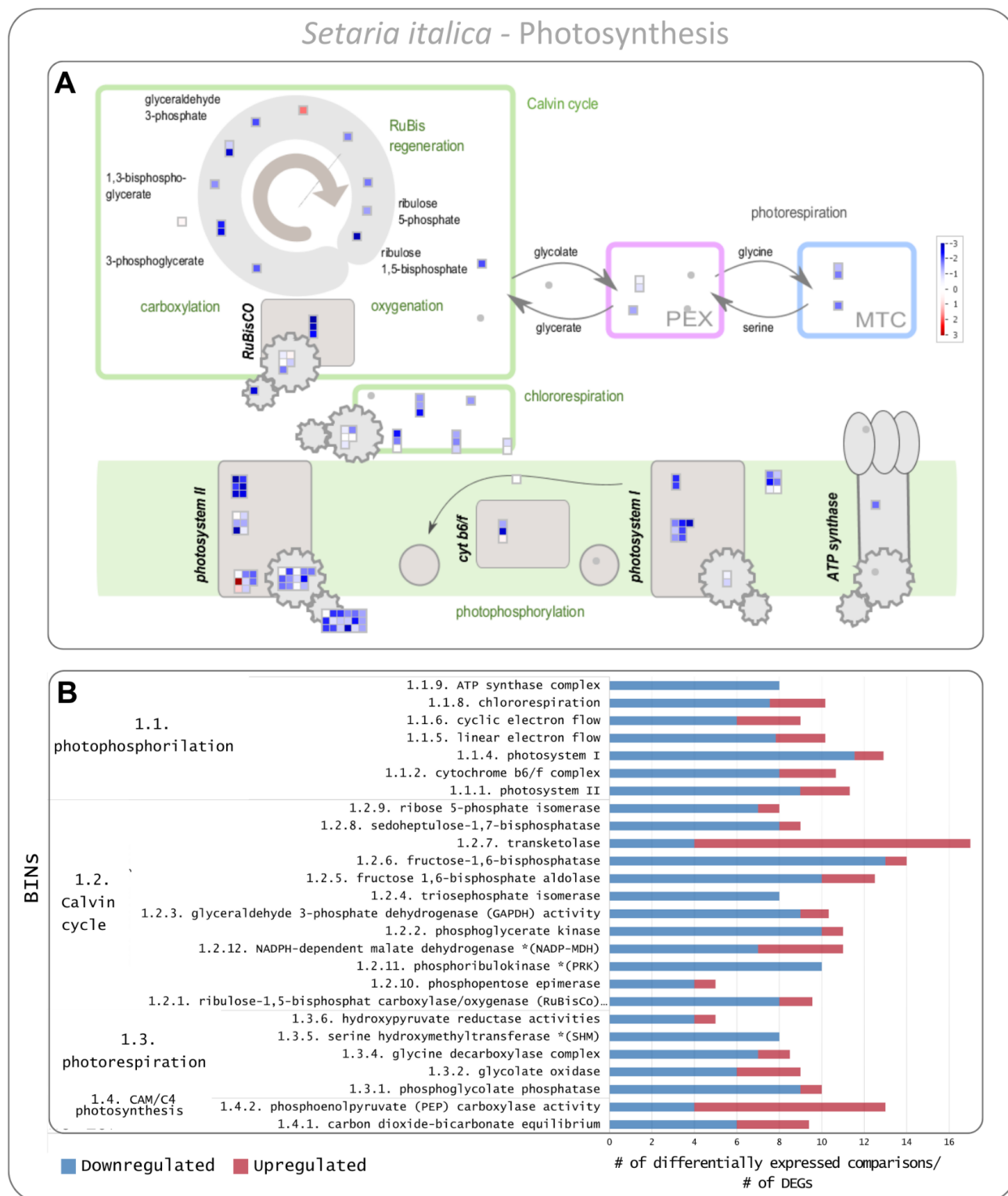


**Figure 6.** Photosynthesis pathway of *S. italica*. Averaged plot of photosynthesis pathway of *S. italica* under abiotic stress (A). Sub-BIN representation analysis of up and downregulated DEGs (B). Only genes differentially expressed in at least 50% of the comparisons were plotted.

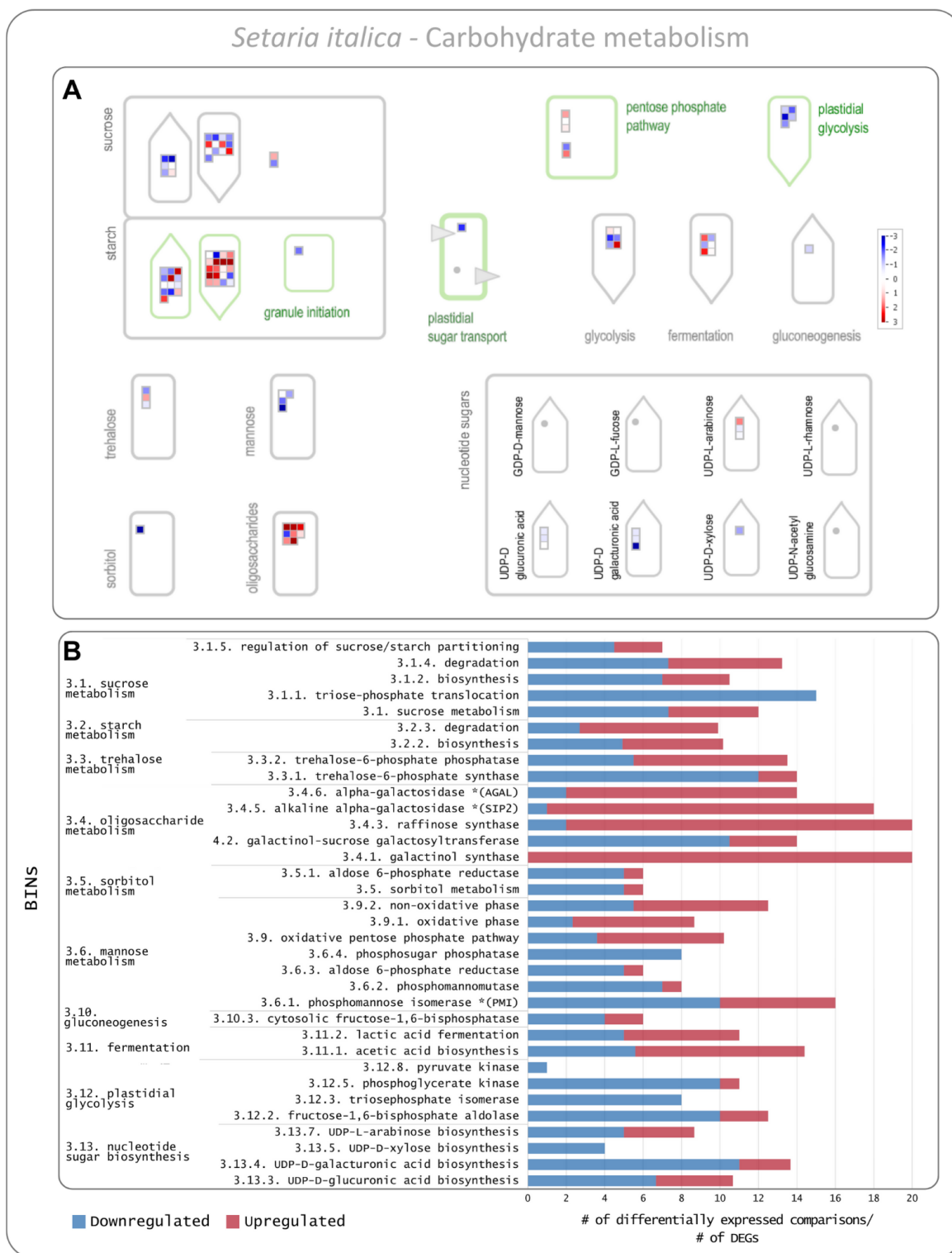


**Figure 7.** Carbohydrate metabolism for *S.italica*. Averaged plot for most frequent DEGs (A). Sub-BIN representation analysis of up and downregulated comparisons (B). Only genes differentially expressed in at least 50% of the comparisons were plotted.

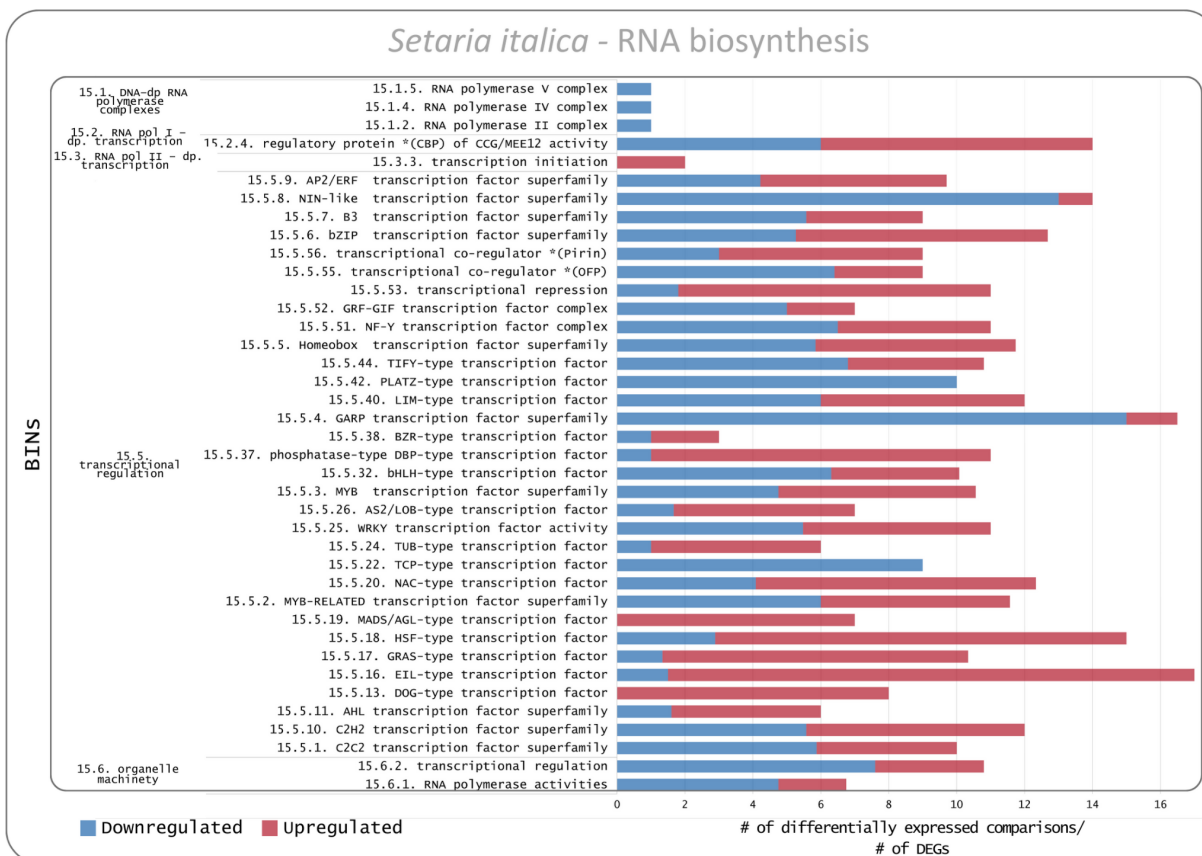


**Figure 8.** Sub-BIN representation analysis of up and downregulated comparisons in the RNA biosynthesis pathway for *S. italica*.

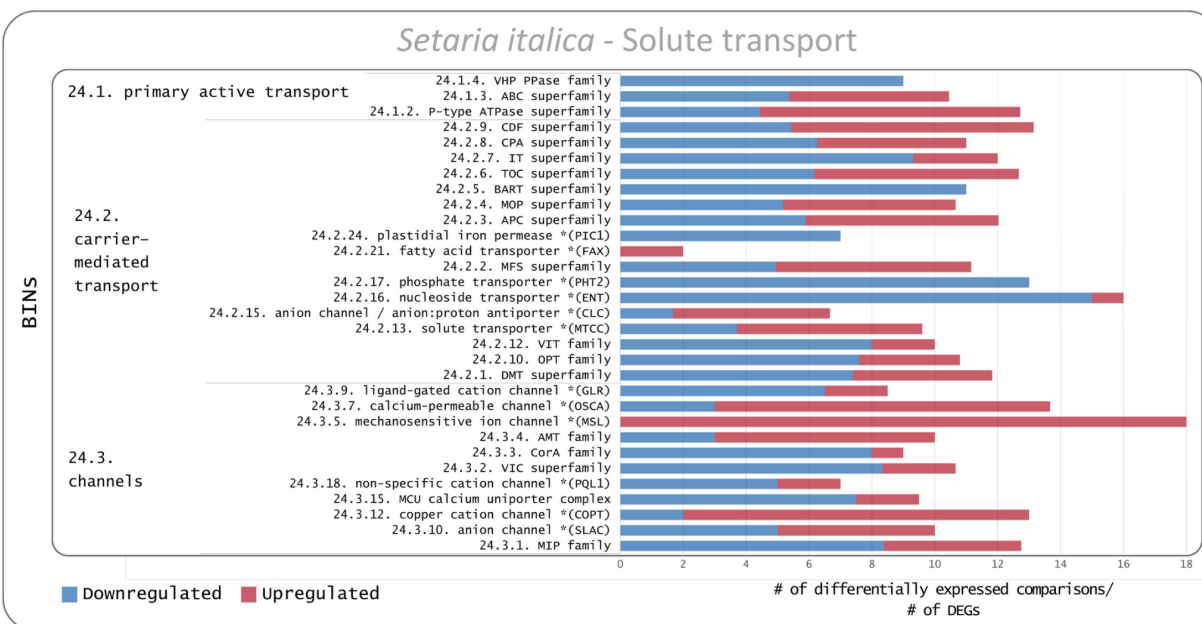


**Figure 9.** Sub-BIN representation analysis of up and downregulated comparisons in the solute transport pathway for *S. italica*.

### 4.3. Functional annotation and representation analysis of *S. viridis*

The Mapman metabolism overview for all DEGs in *S. viridis* also revealed gene expression modulation in various processes and pathways (**Figure 10A**), and this pattern remained consistent even when focusing on the most frequent DEGs (**Figure 10B**). The Mapman plots did not evidence major patterns of up or downregulation in the pathways. The analysis of DEG frequency ratio for *S. viridis* revealed that protein biosynthesis (BIN 17) and carbohydrate metabolism (BIN 3) were the most represented BINs, and RNA biosynthesis (BIN 15) and solute transport (BIN 24) were the BINs with the highest absolute values of DEGs (**Figure 11**).

The sub-BIN representation analysis of protein biosynthesis (BIN 17) revealed that most sub-BINs are downregulated (**Figure 12**). The most represented sub-BIN was translation termination (BIN 17.6.5) and the sub-BIN with highest absolute number of DEGs was ribosome biogenesis (BIN 17.1, n = 185, [S4 - Sevir subBINs](#)), which was largely downregulated. The Mapman plot of carbohydrate metabolism (BIN 03) revealed modulation in various components (**Figure 13A**). The sub-BINs that were most represented were sorbitol dehydrogenase (BIN 3.5.2), which was mostly downregulated, and GDP-mannose biosynthesis (BIN 3.13.1), which was totally upregulated. Oligosaccharide metabolism (BIN 3.4) was less modulated than in *S. italica* (**Figure 13B**), nevertheless, GolS (BIN 3.4.1) and RafS (BIN 3.4.3) remained the highest modulated sub-BINs within oligosaccharide metabolism (BIN 3.4). In terms of RNA biosynthesis (BIN 15) there is a notable prevalence of sub-BIN transcriptional regulation (BIN 15.5), featuring more modulated TF families than *S. italica* (**Figure 14**). Specifically, 411 DEGs were modulated, with 1,116 comparisons being upregulated and 686 downregulated ([S4 - Sevir subBINs](#)). The TF category with highest representation was HSF-type family (BIN 15.5.18). Additionally, we identified downregulation of BINs related to nuclear and organellar RNA transcription, like DNA-dependent RNA polymerase complexes (BIN 15.1), RNA polymerase I-dependent transcription (BIN 15.2), RNA polymerase II-dependent transcription (BIN 15.3), RNA polymerase III-dependent transcription (BIN 15.4) and organelle machinery (BIN 15.6). Finally, solute transport (BIN 24) had the plastidial nitrite transporter (NTR2, BIN 24.2.23) as the most represented sub-BIN, appearing on seven comparisons out of 12 (**Figure 15**) and as mostly

downregulated. The second largest sub-BIN for solute transport was ATM family channels (BIN 24.3.4).

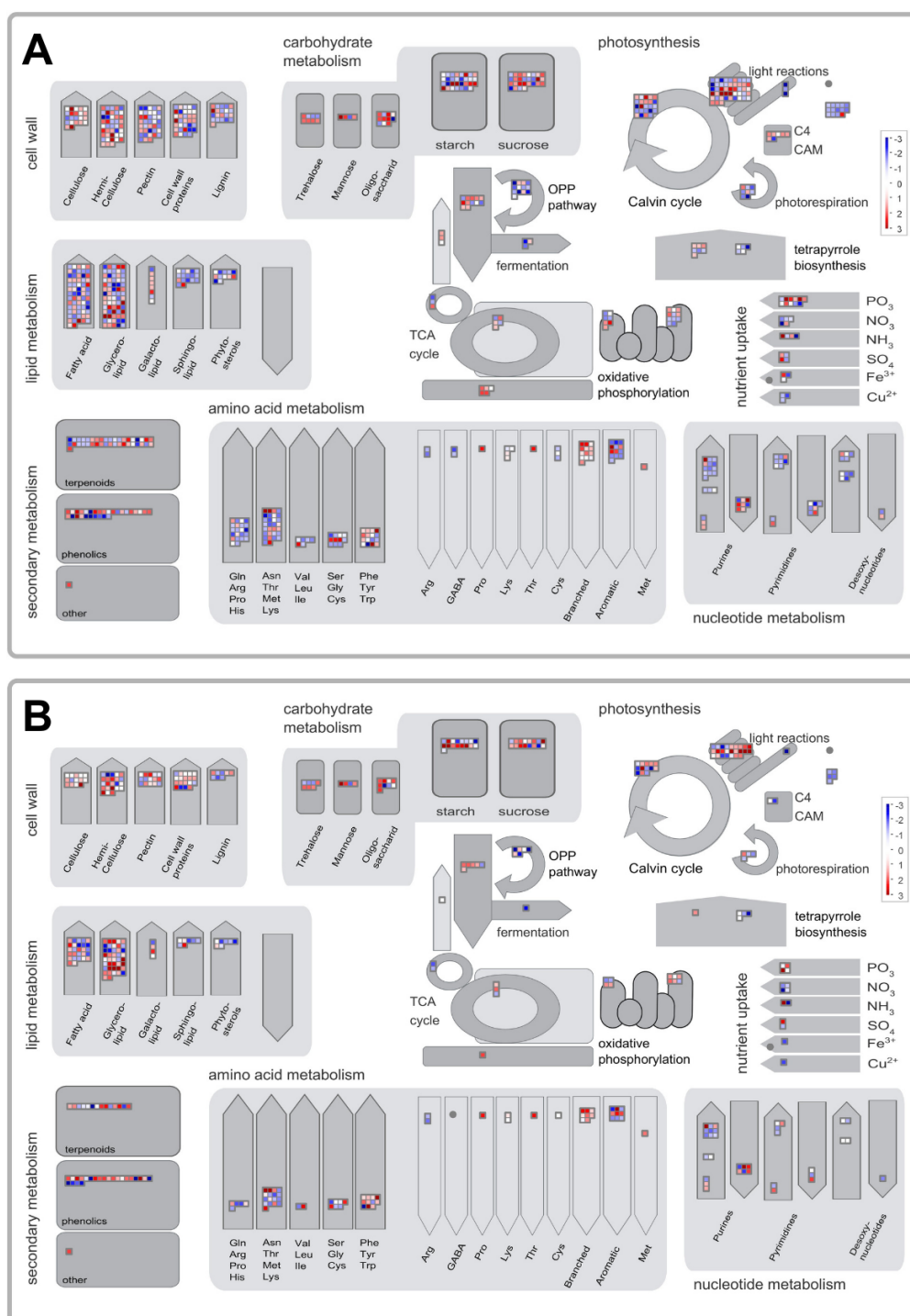


**Figure 10.** Mapman metabolism overview for all DEGs (A) and DEGs present at least in 50% of the comparisons (B) of *S. viridis*, respectively.

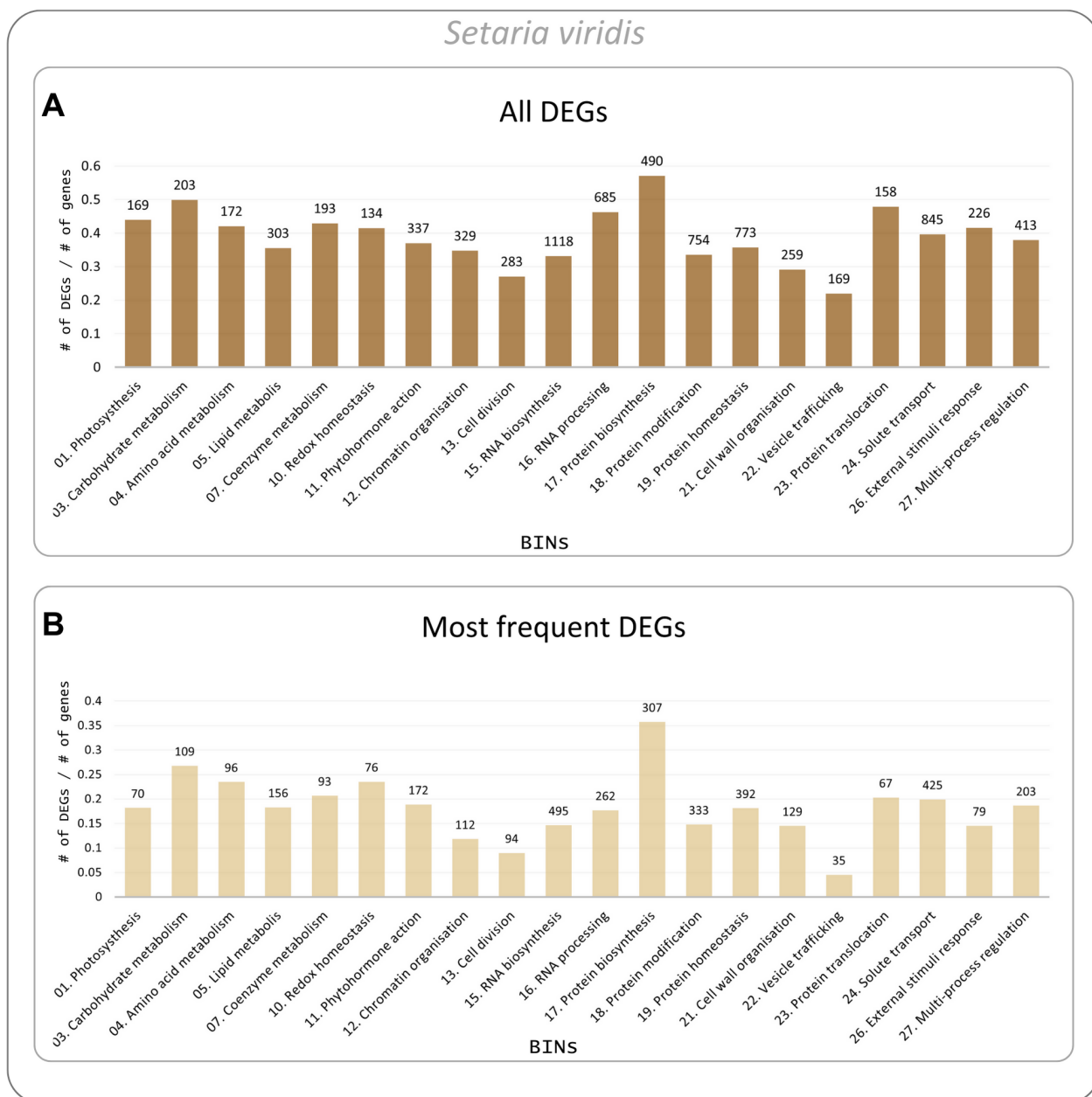


**Figure 11.** DEG frequency ratio across BINS for all DEGs (A) and most frequent DEGs (B) of *S. viridis*, respectively. The upper and bottom graphs show the DEG frequency ratios considering all DEGs (A) and the gene differentially expressed for at least 50% of the comparisons (B), respectively. The absolute numbers of DEGs are shown above each bar. Only BINS with at least 1% of the mapped DEGs were shown.



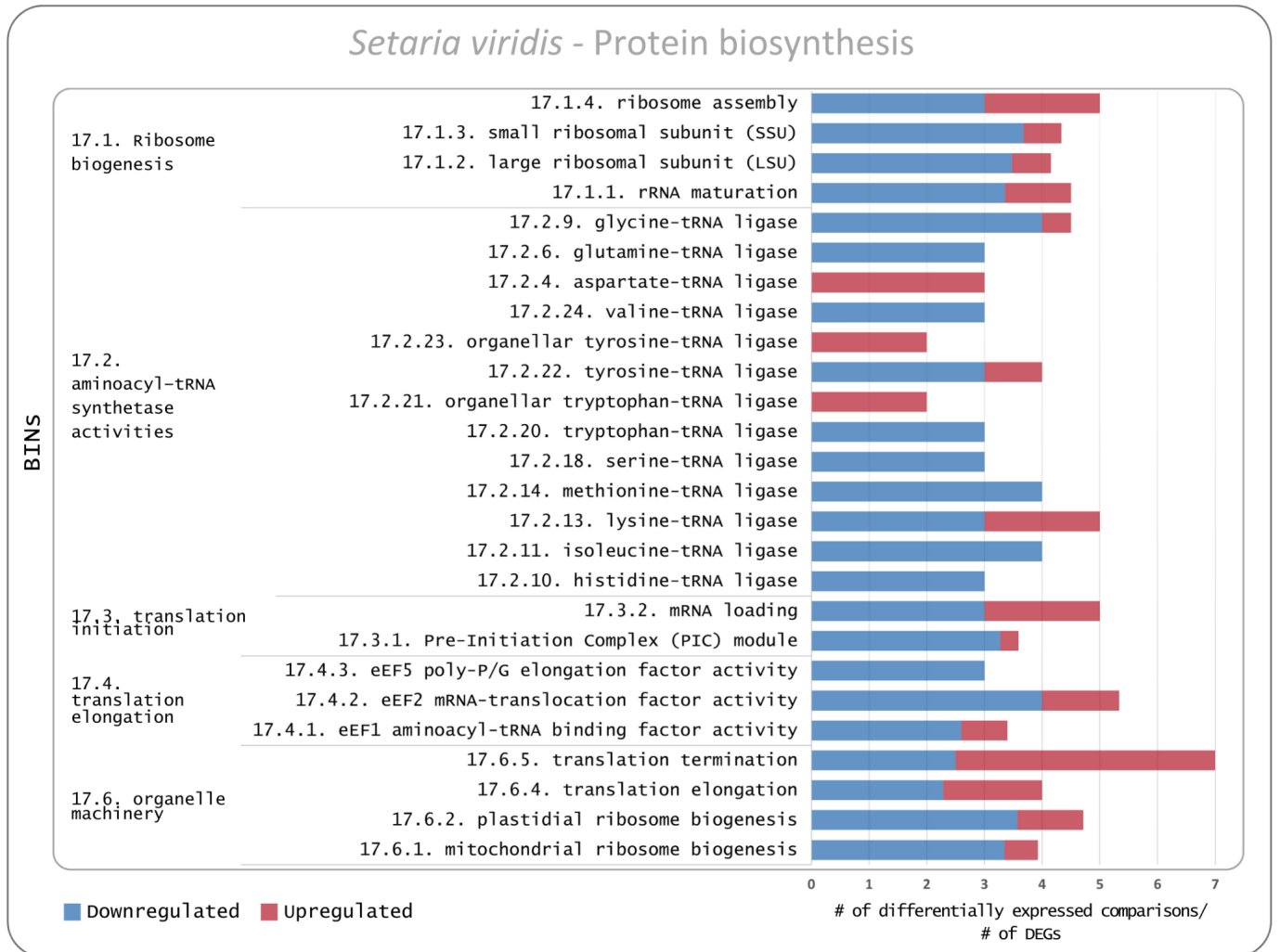


**Figure 12.** Sub-BIN representation analysis of up and downregulated comparisons in the protein biosynthesis pathway for *S. viridis*.

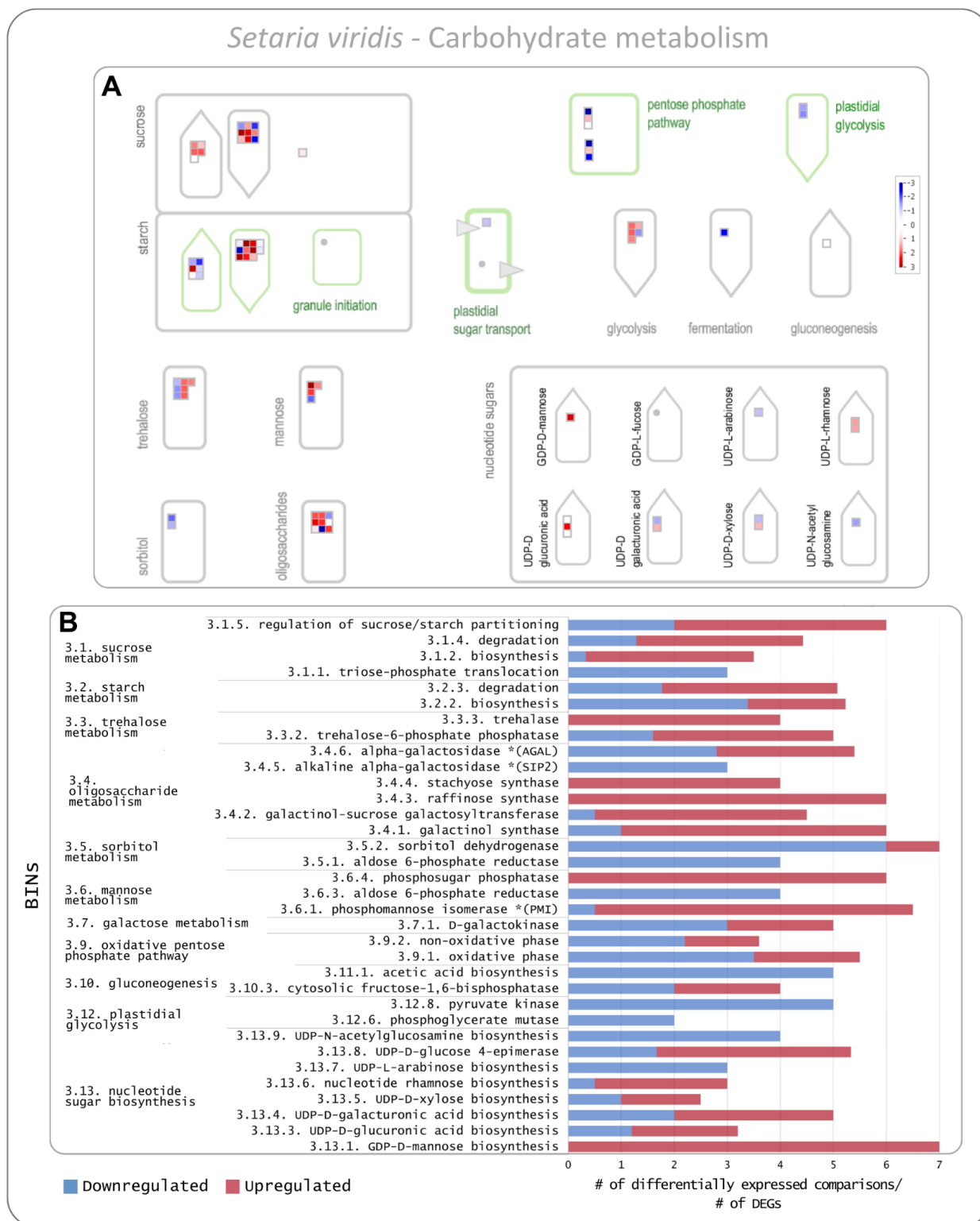


**Figure 13.** Carbohydrate metabolism for *S. viridis*. Averaged plot for most frequent DEGs (A). Sub-BIN representation analysis of up and downregulated comparisons (B).

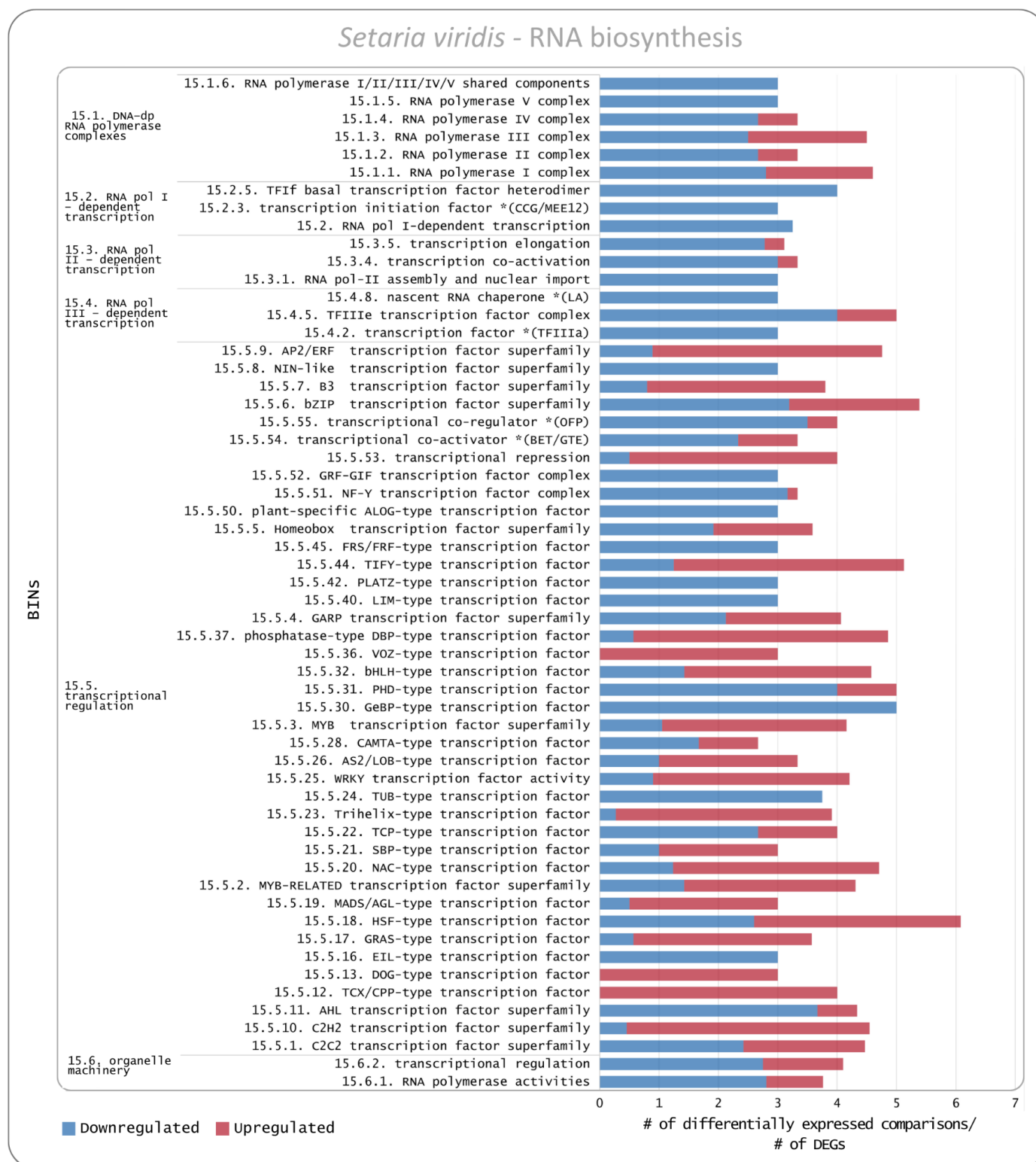


**Figure 14.** Sub-BIN representation analysis of up and downregulated comparisons in the RNA biosynthesis pathway for *S. viridis*.

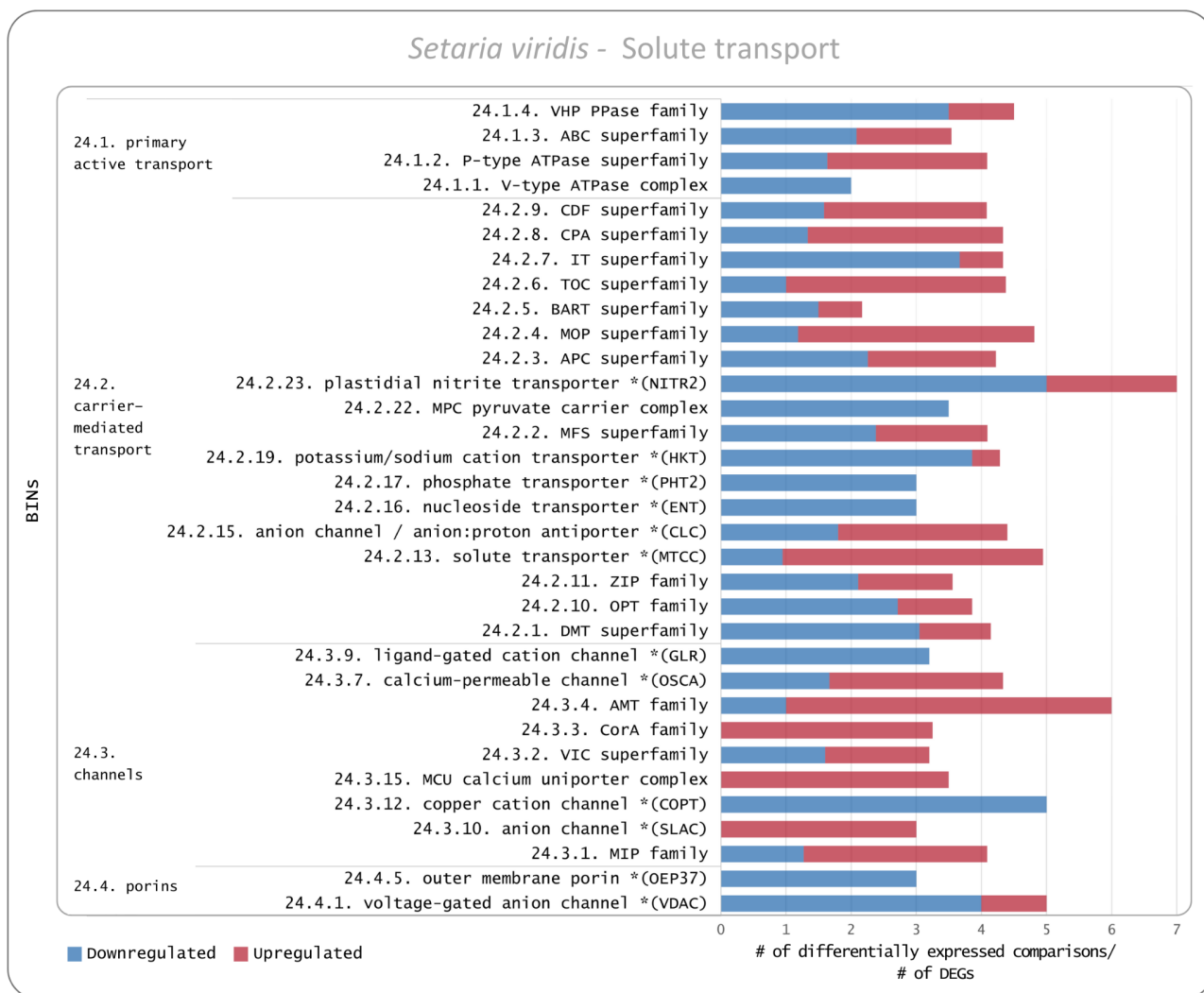


**Figure 15.** Sub-BIN representation analysis of up and downregulated comparisons in the solute transport pathway for *S. viridis*.

#### 4.4. Not functionally annotated genes

Among the genes differentially expressed in more than 50% of the comparisons, a total of 82 genes in *S. italica* and 231 in *S. viridis* were identified as belonging to the BIN 35, which encompassed unannotated genes ([S5 - Unannotated genes](#)). However, 62 and 192 of these DEGs had a gene annotation assignment in the Phytozome database, for *S. italica* and *S. viridis*, respectively. Several of these genes are known to be members of gene families involved with abiotic stress response, as for example Sevir.1G01170 and Sevir.9G281600, which were annotated as late embryogenesis abundant protein (LEA\_2) and E3 ubiquitin-protein ligase (TRIP12) and were modulated in 83% and 67% of comparisons, respectively. Some examples in *S. italica* that were differentially expressed were Seita.3G218800, annotated as protein phosphatase 2C; Seita.4G159500, belonging to seed maturation family proteins; and, and a dehydrin (Seita.8G115400), which is a member of LEA proteins. These last three *S. italica* locus were differentially expressed in 73%, 70% and 67% of the comparisons.

#### 4.5. APX and GPX gene expression modulation in response to abiotic stress

*Setaria italica* and *S. viridis* have 10 and nine *APX* and six and seven *GPX* genes, respectively (V.G.T.B., personal communication). Under drought stress, nine genes encoding *APX* isoenzymes of *S. italica* were modulated in shoot tissue, with both up and downregulation profiles, and five were identified on roots (*SiAPX01*, *SiAPX04*, *SiAPX06*, *SiAPX08* and *SiAPX10*, **Figure 16A**), of which all but one were upregulated. Six out of seven *APX* differentially expressed on root tissue under salt stress (*SiAPX01*, *SiAPX04*, *SiAPX06*, *SiAPX08*, *SiAPX09* and *SiAPX10*) were downregulated, and two *APX* with opposite modulation were found on shoots (*SiAPX01*, *SiAPX07*) under salt stress. Additionally, *SiAPX05*, *SiAPX06* and *SiAPX10* were upregulated on seed tissue. Cold stress downregulated two *APX* genes (*SvAPX02* and *SvAPX08*).

For the *GPX gene family*, all six *S. italica* genes were modulated during drought on shoots tissue, showing both up and downregulation (**Figure 16B**). All *S. italica GPXs* on roots tissue under drought were downregulated (*SiGPX01*, *SiGPX02* and *SiGPX05*). During salt stress, *SiGPX05* was upregulated on both shoots and roots tissue and *SiGPX02* was downregulated on shoots. Additionally, *SiGPX01* and *SiGPX04* were upregulated on seed tissue under salt stress (**Figure 16B**).

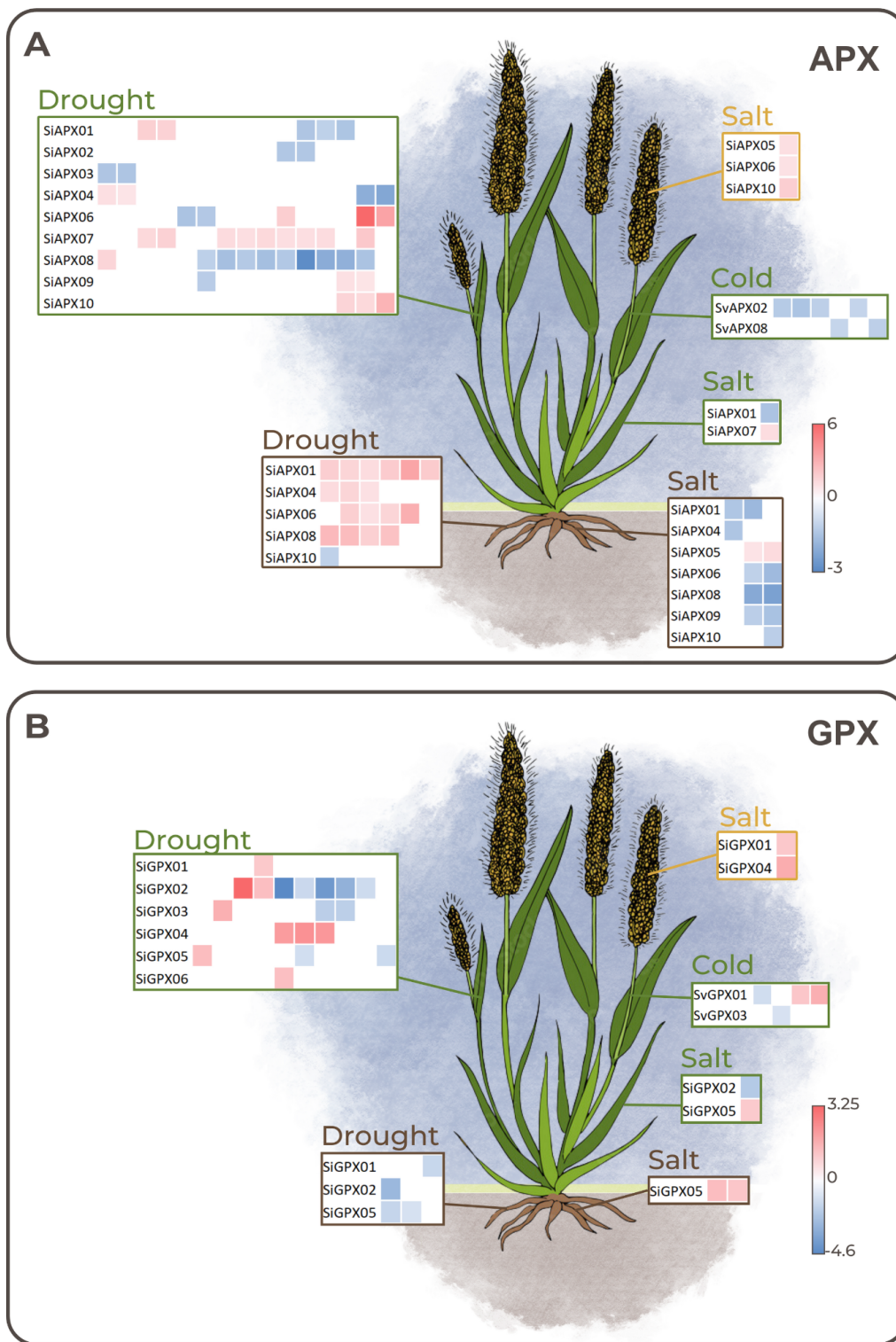


**Figure 16.** Heatmaps of *APX* (A) and *GPX* (B) gene expression profiles (LogFC) in different tissues for *S. italica* and *S. viridis*.

In order to identify networks of co-expression between *APX* and *GPX* genes in our abiotic stress dataset, we calculated similarity Gene Coexpression Networks (GCNs) using all DEGs from *S. italica* submitted to osmotic stress, i.e. drought, salt and PEG-induced stress, as well as all DEGs from *S. viridis* submitted from cold stress. Gene co-expression networks showed no connections between *APXs* and *GPXs*, being these genes also co-expressed with a different set of DEGs from each other (**Figure 17A and B**). Based on the adopted cut-off, GCNs were retrieved for *SiAPX02*, *SiAPX05*, *SiAPX09*, and *SiAPX10* under osmotic stress, i.e. drought, salt and PEG-induced stress, along with *SvAPX02* and *SvAPX08* under cold stress (**Figure 17A**). In the case of *GPX*, two from each species were selected, namely *SiGPX04* and *SiGPX06* for osmotic stress and *SvGPX01* and *SvGPX03* for cold stress (**Figure 17B**). Both *SvAPX02* and *SvGPX06* genes demonstrated GCNs with the highest number of DEGs for each gene family, exhibiting a high  $\rho$  range ( $-0.95 \leq \rho \leq 0.95$ ). The GCNs analysis also revealed that various functional categories were present among the co-expressed genes. Differentially expressed genes related to protein biosynthesis (BIN 17), protein modification (BIN 18) and protein homeostasis (BIN 19) were abundant, with at least one of these categories being present in every GCN created. Other frequently occurring BINs were solute transport (BIN 24), RNA biosynthesis (BIN 15) and RNA processing (BIN 16).

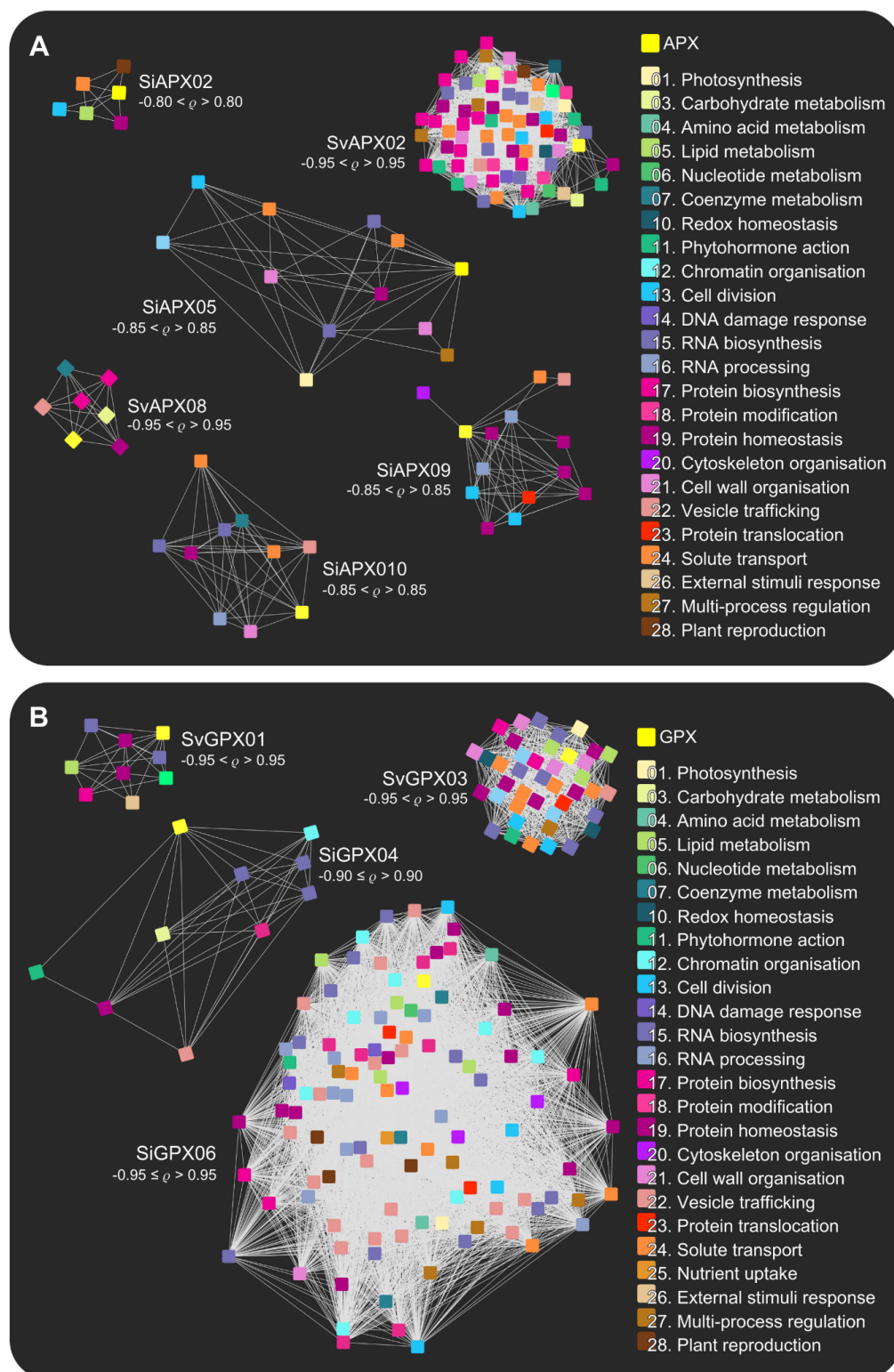


**Figure 17.** Gene co-expression networks (GCNs) for *APX* (A) and *GPX* (B) genes of *S. italica* and *S. viridis*. Each square and line represent a DEG and a significant similarity value between two DEGs, respectively. DEGs were associated with the Mercator BIN functional annotations. *APX*s and *GPX*s are represented in bright yellow. Only *APX* and *GPX* first-neighbor DEGs are shown. Pearson correlation coefficients ( $\rho$ ) are shown below locus names.



## 5. DISCUSSION

Meta-analysis serves as a powerful tool to enhance the robustness and reliability of research outcomes by identifying consistent patterns across diverse experiments ([Ramasamy et al. 2008](#)). This approach elevates statistical strength by capturing prevalent trends across the data. Meta-analysis approaches have been used before to study the transcriptome of wheat under salt, drought, heat and cold stress ([Saidi et al., 2023](#)), of rice under chilling, salt and drought stress ([Buti et al., 2019](#)), of *Arabidopsis* under both biotic and abiotic stress ([Biniiaz et al., 2022](#)) and salt stress ([Zhang et al., 2017](#)) and various crops were studied under cold ([Vergata et al., 2022](#)) and drought stress ([Benny et al., 2019](#)), with the purpose of revealing key genes and pathways for abiotic stress response. Plants respond to stress by sensing external stimuli through receptors on the cell surface and initiating a signaling cascade to alter gene expression in order to adapt to challenging environmental conditions ([Verma et al., 2013](#)). Here, we aimed to analyze the gene expression of responses of *S. italica* and *S. viridis* to different types of abiotic stress using a meta-analysis approach, which had not yet been performed to these plant species. The identification of key pathways and genes that contribute to stress tolerance in these plant species is the first step towards the development of improved crops. Gene-edited crops are a world-wide trend, although regulations are still catching up with this technology and misconceptions are still present in public opinion ([Menz et al., 2020](#)). Under a rapidly-changing climate, resilient crops must become a central component of global food production, with C4 cereals playing a major role ([Pardo et al., 2021](#)).

### 5.1. Global gene expression modulation under abiotic stress

Heatmap analyses provided insights into the overall stress responses of both species. *S. italica* revealed two distinct clusters of predominantly up or downregulated DEGs (**Figure 3A**), indicating similar modulation across different stress conditions and tissues analyzed. Previous studies have indicated the cross-talk between signaling pathways of different stressors such as drought, heat, cold and high salinity. With a large number of genes being commonly induced between various types of abiotic stress ([Verma et al., 2013](#)). Accordingly, we identified that drought stress shared 97% and 88% of its most expressed DEGs with PEG-induced and salt stress DEGs, respectively (**Figure 2**). Notably, the *S. italica* analyzed stress types are all related

to osmotic stress. Indeed, it has been reported before that there is an overlapping of pathways and metabolite response between salt and drought stress ([Ma et al., 2020](#)). These stressors also display a similar early response, causing a decrease in stomatal aperture, photosynthetic impairment, reduction in growth and nutrient deficit ([Ma et al., 2020](#)). Plants submitted to salt stress for longer periods also experience ionic stress ([Chaves et al., 2009](#)), and known mechanisms of drought response in plants include closing of stomata and decreased transpiration rate, suppression of photosynthesis and cell growth, decrease in osmotic potential of plant tissues and increase in respiration ([Suguiyama et al., 2022](#); [Verma et al., 2013](#)).

*Setaria italica*'s heatmap divided the comparisons, i.e. RNA-seq experiments, in two main clusters that were further divided into two sub-clusters each. One cluster divided comparisons by tissue, indicating tissue-specific responses that can be explained by the different functions of each tissue (**Figure 3A**). Roots and shoots tissues respond to abiotic stress differently ([Hazen et al., 2003](#)), with metabolism-related proteins playing specific roles in each organ in order to achieve adaptation ([Verma et al., 2013](#)). Specifically during drought, root elongation is enhanced as the plant searches for water underground, while shoots growth is inhibited due to energy conservation ([Hazen et al., 2003](#)). This cluster did not separate stress types, even though it is possible to note a predominance of drought comparisons. On the other hand, the left cluster did not divide tissue nor stress types (**Figure 3A**). This cluster was probably formed due to the low number of DEGs identified for those comparisons, including the comparisons of seed tissue.

The heatmap analysis of *S. viridis* revealed that cold stress exhibited more DEGs than other analyzed stresses, as well as a different set of DEGs than those present on heat and high light stress (**Figure 3B**). This outcome is unsurprising, considering that heat stress and cold stress represent diametrically opposing conditions, thereby evoking distinct molecular reactions ([Li et al., 2020](#)). Furthermore, we identified a cluster of DEGs predominantly expressed during high light stress (**Figure 3B**), which displayed only a modest overlap with cold stress DEGs. This observation is consistent with the inherent dissimilarities between high light stress and cold stress, being the first characterized by solar radiation exposure and therefore often associated with heat stress ([Anderson et al., 2021](#)). Their limited gene overlap aligns with the fundamental distinctions that define these stress types in terms of molecular responses, pathways, and modulated genes ([Li et al., 2020](#)).

In both species, modulation across all components in metabolism overview was evident both for all and most frequent sets of DEGs (**Figure 4 and 10**). Interestingly, *S. italica* modulates a greater number of genes than *S. viridis* (**Table 1**), this disparity can be attributed to the quantity of comparisons analyzed in each species. As the number of comparisons increases, the potential for unique genes to appear in each comparison also grows. On the other hand, if we consider only genes differentially expressed in more than 50% of the comparisons, *S. italica* displays fewer DEGs than *S. viridis* (**Table 1**), since it becomes progressively more challenging for genes to be consistently shared across all of these comparisons as the number of comparisons grow. The approach of filtering the database by DEGs expressed in at least half of the comparisons for each type of stress enables us to select a set of more relevant candidate genes responsible for the abiotic stress response in *Setaria* spp.

Photosynthesis is known to be one of the first processes to be affected by drought or salt stress, with drought being particularly detrimental ([Muhammad et al., 2021](#); [Nouri et al., 2015](#)). Several studies have shown that genes associated with photosynthesis are downregulated in response to salt and drought stress ([Suguiyama et al., 2022](#); [Nouri et al., 2015](#); [Chaves et al., 2009](#)). Aligning with these findings, our analysis uncovered a consistent downregulation of photosynthesis (BIN 1) across the majority of our comparisons (**Figure 6**). The downregulation of genes associated with photosynthesis in osmotic stress conditions can be understood as a primary response to stomata closure upon dehydration, thus preventing evapotranspiration and further water loss ([Golldack et al., 2014](#); [Chaves et al., 2003](#)). Stomatal closure is not only a mechanical response but is also dependent on intricate regulatory pathways ([Golldack et al., 2014](#)). Carbon uptake is impaired by stomatal closure and the scarcity of carbon substrates leads to the inhibition of Rubisco and reduction of ATP synthesis ([Chaves et al., 2003](#)). ATP synthase, PSI and PSII have been extensively described to be downregulated during stress response ([Nouri et al., 2015](#)). All of these components were found to be downregulated in our comparisons, with Rubisco being greatly affected (**Figure 6A**).

The sub-BINs representation analysis for carbohydrate metabolism (BIN 3) under osmotic stress revealed that for *S. italica* oligosaccharides metabolism (BIN 3.4) was the most representative sub-BIN throughout our comparisons (**Figure 7B**). Among oligosaccharides metabolism, GolS (BIN 3.4.1) and RafS (BIN 3.4.3) were the most prominent sub-BINs, both being modulated in 20 out of 37 comparisons ([S3 - Seita sub-BINs](#)). GolS was upregulated in all

comparisons while RafS in 18. GolS is a key enzyme for raffinose metabolism, being involved in the first step of its biosynthesis ([ElSayed et al., 2012](#)). Upregulation of GolS is associated with abiotic stress response, and it's been proposed that different isoforms are related to different kinds of stress ([ElSayed et al., 2012](#)). Growing evidence suggests raffinose improves seed desiccation tolerance, contributing to resistance against drought stress, and also accumulates in leaves and roots acting in protection mechanisms ([Xu et al., 2023](#)). Various studies have demonstrated that during stress conditions raffinose accumulation is increased to compensate for the rise in ROS ([Xu et al., 2023](#)). Evidence of a study that analyzed expression pattern of RafS in grasses, including the species *Brachypodium distachyon*, *Brachypodium stacei*, *Oropetium thomaeum*, *Oryza sativa*, *Panicum hallii*, *Panicum virgatum*, *S. italica*, *S. viridis*, *Sorghum bicolor* and *Zea mays* revealed that most of *RafS* genes were up-regulated under drought and salt stress, strongly pointing to a participation in these plants adaptation ([Xu et al., 2023](#)). It has been shown that transgenic *Arabidopsis* plants with increased galactinol and raffinose concentrations had better ROS scavenging capacity ([ElSayed et al., 2012](#)). GolS and RafS were also majoritarily upregulated in *S. viridis* under temperature and high light stress conditions, although they weren't the most representative sub-BINs (**Figura 13B**).

Protein biosynthesis (BIN 17) was the most prominent BIN of *S. viridis* in response to temperature and high light stress and was found to be mostly downregulated (**Figure 12**). Protein biosynthesis is an energetically expensive process, and its adequate regulation in response to stress is essential. In this context, tRNAs play a key role in the translational reprogramming ([Advani and Ivanov, 2019](#)). Our investigation identified modulation within several tRNA families (BIN 17.2, **Figure 12**), although the majority were not included in the most representative BINs. Translation initiation impairment is a known hallmark of stress-induced translational control ([Advani and Ivanov, 2019](#)), in our results this sub-BIN was mostly downregulated (BIN 17.3), much like ribosome biogenesis (BIN 17.1), also a major player in protein biosynthesis ([Advani and Ivanov, 2019](#)). These results point to a decreased translation in *Setaria* spp. during temperature stress response.

Regarding the responses to temperature and high light stress of *S. viridis* carbohydrate metabolism, two significant sub-BINs stood out: the upregulation of sorbitol dehydrogenase (BIN 3.5.2) and the downregulation of GDP-mannose biosynthesis (BIN 3.13.1, **Figura 13B**). Plants accumulate different kinds of osmolytes like sorbitol and trehalose in response to abiotic

stress ([Verma et al., 2013](#)). Sorbitol dehydrogenase has been associated with the response to abiotic stress in *A. thaliana* and grapevine ([Jia et al., 2015](#)). Interestingly, it didn't feature in *S. italica's* carbohydrate metabolism in our dataset of osmotic stress. Previous studies have demonstrated that overexpression of an *Medicago sativa* GDP-mannose 3,5-epimerase in transgenic *Arabidopsis* resulted in improved acid, drought, and salt tolerance by enhancing ascorbate accumulation ([Ma et al., 2020](#)).

In both *S. italica* and *S. viridis*, the category of RNA biosynthesis (BIN 17) exhibited the highest absolute count of DEGs (**Figures 8 and 14**), a notable indication of its significance in response to abiotic stress. Transcription factors respond to a signaling cascade initiated by perception of stimuli and act inhibiting or enhancing the expression of stress-responsive genes ([Verma et al., 2013](#)). Frequently, a single TF is responsible for modulating the expression of multiple genes ([Saidi et al., 2023](#)). Notably, both species demonstrated pronounced modulation across various families of transcription factors (TFs), although *S. viridis* displayed a broader array of modulated families (**Figures 8 and 14**). In fact, *S. viridis* displayed 73,19% more genes in RNA biosynthesis than *S. italica*. It has been reported that acclimatization to cold involves massive transcriptome reprogramming ([Verma et al., 2013](#)), which suggest the cross-talk of several pathways in this stress response. Previous works on *S. italica* identified that TFs such as bZIP, ERF, HB-other, HD-ZIP, MYB, NAC and WRKY were responsive during drought stress ([Qi et al. 2013](#); [Suguiyama et al., 2022](#)). In our analysis, the WRKY (BIN 15.5.25), MYB (BIN 15.5.3), bZIP (BIN 15.5.3) and ERF (BIN 15.5.9) superfamilies were all observed to be modulated in both species. WRKY has been reported to participate in linking ROS scavenging to osmotic and oxidative stress by targeting peroxidases ([Golldack et al., 2014](#), [Miller et al., 2010](#)). Specifically, the EIL-type (BIN 15.5.16) transcription factor emerged as a significant sub-category within the RNA biosynthesis of *S. italica* (**Figure 8**), exhibiting predominantly upregulated expression. Intriguingly, in *S. viridis*, this sub-category displayed complete downregulation (**Figure 14**). The EIL family is involved in ethylene signaling pathways that regulate several developmental as well as defense processes ([Li et al., 2019](#)). In *S. viridis*, the sub-BIN with highest representation was the HSF family (BIN 15.5.18). HSF transcription factor family is involved in acquired thermotolerance and linked to heat stress response ([Myers et al., 2023](#)).

Solute transport (BIN 24) emerged as the second highest BIN with the highest absolute count of DEGs for both *S. italica* and *S. viridis* (**Figures 9 and 15**). Notably, within this, the mechanosensitive channel (BIN 24.3.4) exhibited an upregulated expression in *S. italica* (**Figure 9**), while interestingly, it did not manifest in *S. viridis* (**Figure 15**). Mechanosensitive channels are related to perceiving vital mechanical stimuli, including osmotic pressure ([Basu et al., 2017](#)). Mechanosensitive ion channels in plants have been recognized to contribute to cell and organelle osmoregulation, as well as root mechanosensing ([Basu et al., 2017](#)). *Setaria viridis* presented the BIN 24.2.23 (NITR2) as the most frequent sub-BIN in solute transport. Recent studies have unveiled the extensive involvement of NITR2 (Nitrate Transporter 2) in dealing with adverse environmental conditions, beyond its role in managing limited nitrate/nitrogen availability ([Zhang et al., 2018](#)).

In our analysis we came across several genes that were differentially expressed in most of the comparisons, but were not mapped to the Mercator tool, being assigned to the unannotated category (BIN 35) ([S5 - Unannotated genes](#)). These unannotated DEGs represent an intriguing aspect of the study, as they might have important roles in the biological processes under investigation, yet they are uncategorized in functional groups. On the other hand, several of these genes were already annotated in the Phytozome database and were described as related to *Arabidopsis* and rice genes previously related to the abiotic stress response, as for example Sevir.1G01170, Seita.4G159500 and Seita.8G115400, which belongs to the late embryogenesis abundant protein (LEA) family. LEA proteins are known as an important player in damage repair during abiotic stress, and they are activated mostly by Ca<sup>2+</sup>-dependent signaling molecules ([Nagaraju et al., 2019](#)). DEGs related to protein modification like Sevir.9G281600 (E3 ubiquitin-protein ligase (TRIP12)) and Seita.3G218800 (Protein phosphatase 2C) were also identified. Protein ubiquitination participates in protein degradation, with ubiquitin ligases being crucial to substrate recognition ([Wange et al., 2022](#)). Ubiquitin ligase (E3) are known to participate in regulation of drought response ([Jia et al., 2015](#)). Protein phosphatases 2C are widely important in many signaling pathways, as protein phosphorylation is a universal post-translational modification ([He et al., 2019](#)).

Overall, we can understand that the plant's response to abiotic stress is a result of modulation in diverse pathways, with cross-talk between diverse cellular compartments. Response to stress starts as perception of signal through various membrane receptors ([Verma et](#)

[al., 2013](#)) such the MLS channel here identified. The membrane receptors through varying cytoplasmic  $\text{Ca}^{2+}$  levels generate secondary signaling molecules that initiate protein phosphorylation cascades that further activate TFs ([Verma et al., 2013](#)), such as EIL and HSF. At last, TF activates or inhibits stress-responsive genes, amongst which we can mention the LEA gene family.

## 5.2. APX and GPX gene expression modulation under abiotic stress

Oxidative signaling stands at the core of the intricate networks orchestrating plant responses to stress ([Noctor et al., 2014](#)). Abiotic stressors such as drought, salinity, intense light exposure, and elevated temperatures are known to generate ROS ([Miller et al., 2010](#)). Accordingly, ROS-scavenger mechanisms have been reported to participate in resistance against those stressors ([Miller et al., 2010](#)). ROS are produced in various cell compartments even under normal circumstances as by-products of various metabolic processes ([Shigeoka et al., 2002](#)). ROS are often formed from transfer of high-energy electrons to water and oxygen molecules ([Miller et al., 2010](#)). This accumulation of electric charges can be explained by the impairment of the electron transport chain in both chloroplast and mitochondria, and can be a consequence of limitation of  $\text{CO}_2$  fixation in photosynthesis during stress situations ([Miller et al., 2010](#)). The implications of excessive ROS are profound, as they hold the potential to inflict damage upon cellular membranes, disrupting the delicate balance of ion homeostasis within plants ([Dortje et al., 2014](#)), they can also damage proteins, nucleic acids and lipids ([Miller et al., 2010](#)). Therefore, maintaining the right balance of ROS is crucial for determining plant survival in response to adverse conditions.

ROS levels are meticulously regulated through the interplay of antioxidant metabolites and ROS detoxifying enzymes ([Dortje et al., 2014](#)). The removal of excessive ROS is primarily achieved through enzymatic and non-enzymatic mechanisms, where the non-enzymatic components receive the excessive levels of ROS and function as an antioxidant buffer and the specialized enzymes actively scavenge and eliminate ROS ([Miller et al., 2010](#)). The major ROS-scavenging enzymes in plants are superoxide dismutase (SOD), ascorbate peroxidase (APX), catalase (CAT), glutathione peroxidase (GPX), and peroxiredoxin (PrxR) ([Miller et al., 2010](#)). These enzymes play a pivotal role in maintaining ROS homeostasis ([Mittler et al., 2004](#)). Peroxidases, crucial components of this defense system, are categorized into two main groups:

heme-based and thiol-based peroxidases ([Noctor et al., 2014](#)) APX belongs to the heme peroxidase superfamily in plants, while GPX is part of the thiol-based peroxidase family ([Noctor et al., 2014](#)). APX catalyzes the conversion of  $H_2O_2$  into  $H_2O$ , employing ascorbate as an electron donor ([Saurabh et al., 2017](#)), while GPX uses reduced glutathione ([Margis et al., 2008](#)). APXs are particularly important to  $H_2O_2$  removal during photorespiration ([Noctor et al., 2014](#)).

According to Saurabh and collaborator ([2017](#)), different APX isoforms are modulated differently in response to different abiotic stress, influenced by stage of development, subcellular localization and by the presence of specific regulatory elements in the upstream regions of the respective genes. The same APX isoform can also be differentially modulated in different tissues in response to the same kind of stress ([Akbudak et al., 2018](#)). In our analysis, all *APX* and *GPX* genes were modulated in at least one comparison in *S. italica*. Two APXs (SvAPX02 and SvAPX08) and two GPX (SvGPX01 and SvGPX03) were modulated in *S. viridis*. This can be a consequence of the stress types analyzed and the quantity of comparisons used in each species and stress types. Interestingly, on shoots tissue during drought stress SiAPX01, SiAPX04, SiAPX06, SiAPX08 and SiAPX09 were upregulated in some comparisons, while in others they showed opposite modulation. This variability could be attributed to variations in the cultivars, developmental stage or experimental conditions employed across different published studies used in our database. The *GPXs* were also up and downregulated during drought on shoots tissue, although, contrasting with *APX*, on roots all were downregulated.

Coexpression networks are applied to identify genes with similar expression profiles. In this study, we used them to understand whole-genome gene expression modulation associated with our individual *APX* and *GPX* genes of interest. Coexpression, in this context, does not necessarily imply direct protein-protein interactions; rather, it indicates that these genes are modulated together and can exhibit correlations in their expression profiles ([Usadel et al., 2009](#)). The coexpression network analysis revealed that four *S. italica* and two *S. viridis* *APXs* and two *GPXs* of each species were clustered within distinct networks (**Figure 17**), supporting that these genes may present unique responses, different from other gene family members and therefore, a single expression pattern cannot be expected for all locus of *APX* or *GPX* in the whole plant under abiotic stress.

The analysis also showed that various functional categories were present among the coexpressed genes. DEGs related to protein biosynthesis (BIN 17), protein modification (BIN



18) and protein homeostasis (BIN 19) were abundant, with at least one of these categories being present in every network created (**Figure 17**). Other frequently occurring BINs were RNA biosynthesis (BIN 15) and processing (BIN 16) and solute transport (BIN 24). This is expected during transcriptional reprogramming associated with response to stress, as RNA biosynthesis and processing is crucial to the formation of transcription factors and proteins. TFs act as a bridge between sensing stimuli and responding to it, inhibiting or enhancing the expression of stress-responsive genes ([Verma et al., 2013](#)). Protein modification, including phosphorylation, are widely important to the activation and inhibition of all kinds of enzymes ([He et al., 2019](#)). In this way, it is expected that during abiotic stress response these functional categories will be enriched and interact with enzymes, metabolites and genes.

## 6. CONCLUSIONS

The meta-analysis here conducted can contribute to a greater understanding of abiotic stress response in *Setaria* species. We produced a catalog of consistent and likely relevant genes that may participate in the abiotic stress response of *S. italica* and *S. viridis*. Those genes are important candidates for further studies on functional genomics and genetic breeding for abiotic stress and, even climate change conditions, resilience. The elucidation of the intricate networks through which these resilient plants react to environmental cues is imperative for the development of robust crop cultivars capable of thriving in the face of our continuously changing climate. Although, it is important to mention that genetic modification must account for the whole stress-response system in the fields, where abiotic tolerance must be understood as a part of a process of relationships with the environment, the microbiome and other surrounding interacting living beings.

## REFERENCES

ADVANI, V. M.; IVANOV, P. Translational control under stress: reshaping the translome. **BioEssays**, v. 41, n. 5, p. 1900009, 26 apr. 2019. Available at: <<https://doi.org/10.1002%2Fbies.201900009>>

AKBUDAK, M. A. et al. Genome-wide identification and expression profiling of ascorbate peroxidase (*APX*) and glutathione peroxidase (*GPX*) genes under drought stress in sorghum (*Sorghum bicolor L.*). **Journal of Plant Growth Regulation**, v. 37, n. 3, p. 925–936, 14 feb. 2018. Available at: <<https://doi.org/10.1007/s00344-018-9788-9>>

ANDERSON, C. M. et al. High light and temperature reduce photosynthetic efficiency through different mechanisms in the C4 model *Setaria viridis*. **Communications Biology**, v. 4, n. 1, 16 sep. 2021. Available at: <<https://doi.org/10.1038/s42003-021-02576-2>>

BASU, D.; HASWELL, E. S. Plant mechanosensitive ion channels: an ocean of possibilities. **Current Opinion in Plant Biology**, v. 40, p. 43–48, dec. 2017. Available at: <<https://doi.org/10.1016/j.pbi.2017.07.002>>

BENNY, J. et al. Identification of key genes and its chromosome regions linked to drought responses in leaves across different crops through meta-analysis of RNA-Seq data. **BMC Plant Biology**, v. 19, n. 1, 10 may 2019. Available at: <<https://doi.org/10.1186/s12870-019-1794-y>>

BINIAZ, Y. et al. Meta-analysis of common and differential transcriptomic responses to biotic and abiotic stresses in *Arabidopsis thaliana*. **Plants**, v. 11, n. 4, p. 502, 12 feb. 2022. Available at: <<https://doi.org/10.3390/plants11040502>>

BORETTI, A.; ROSA, L. Reassessing the projections of the World Water Development Report. **Npj Clean Water**, v. 2, n. 1, 31 jul. 2019. Available at: <<https://www.nature.com/articles/s41545-019-0039-9>>

BRUTNELL, T. P. et al. *Setaria viridis*: A model for C4 photosynthesis. **The Plant Cell**, v. 22, n. 8, p. 2537–2544, aug. 2010. Available at: <<https://doi.org/10.1105/tpc.110.075309>>

BUTI, M. et al. A meta-analysis of comparative transcriptomic data reveals a set of key genes involved in the tolerance to abiotic stresses in rice. **International Journal of Molecular Sciences**, v. 20, n. 22, p. 5662, 12 nov. 2019. Available at: <<https://doi.org/10.3390/ijms20225662>>

CHAVES, M. M.; FLEXAS, J.; PINHEIRO, C. Photosynthesis under drought and salt stress: regulation mechanisms from whole plant to cell. **Annals of Botany**, v. 103, n. 4, p. 551–560, 28 jul. 2008. Available at: <<https://doi.org/10.1093/aob/mcn125>>

CHAVES, M. M.; MAROCO, J. P.; PEREIRA, J. S. Understanding plant responses to drought — from genes to the whole plant. **Functional Plant Biology**, v. 30, n. 3, p. 239–264, 2003. Available at: <<https://doi.org/10.1071/fp02076>>

DA, Z. et al. Transcriptome analysis reveals key genes in response to salinity stress during seed germination in *Setaria italica*. **Environmental and Experimental Botany**, v. 191, p. 104604–104604, 1 nov. 2021. Available at: <<https://doi.org/10.1016/j.envexpbot.2021.104604>>

DE FRAITURE, C.; WICHELS, D. Satisfying future water demands for agriculture. **Agricultural Water Management**, v. 97, n. 4, p. 502–511, apr. 2010. Available at: <<https://doi.org/10.1016/j.agwat.2009.08.008>>

DOUST, A. N. et al. Foxtail Millet: a sequence-driven grass model system: Figure 1. **Plant Physiology**, v. 149, n. 1, p. 137–141, jan. 2009. Available at: <<https://doi.org/10.1104/pp.108.129627>>

ELSAIED, A. I.; RAFUDEEN, M. S.; GOLLDACK, D. Physiological aspects of raffinose family oligosaccharides in plants: protection against abiotic stress. **Plant Biology**, v. 16, n. 1, p. 1–8, 12 aug. 2013. Available at: <<https://doi.org/10.1111/plb.12053>>

GARG, R.; VARSHNEY, R. K.; JAIN, M. Molecular genetics and genomics of abiotic stress responses. **Frontiers in Plant Science**, v. 5, 21 aug. 2014. Available at: <<https://doi.org/10.3389/fpls.2014.00398>>

GOLLDACK, D. et al. Tolerance to drought and salt stress in plants: Unraveling the signaling networks. **Frontiers in Plant Science**, v. 5, 22 apr. 2014. Available at: <<https://doi.org/10.3389/fpls.2014.00151>>

GOODSTEIN, D. M. et al. Phytozome: a comparative platform for green plant genomics. **Nucleic Acids Research**, v. 40, n. D1, p. D1178–D1186, 22 nov. 2011. Available at: <<https://doi.org/10.1093/nar/gkr944>>

GOWIK, U.; WESTHOFF, P. The path from C3 to C4 photosynthesis. **Plant Physiology**, v. 155, n. 1, p. 56–63, 12 oct. 2010. Available at: <<https://doi.org/10.1104/pp.110.165308>>

GUO, Y. et al. Comparative transcriptomics reveals key genes contributing to the differences in drought tolerance among three cultivars of foxtail millet (*Setaria italica*). **Plant Growth Regulation**, v. 99, n. 1, p. 45–64, 19 jul. 2022. Available at: <<https://doi.org/10.1007/s10725-022-00875-0>>

HAN, F. et al. Transcriptome analysis reveals molecular mechanisms under salt stress in leaves of Foxtail Millet (*Setaria italica* L.). **Plants**, v. 11, n. 14, p. 1864–1864, 18 jul. 2022. Available at: <<https://doi.org/10.3390/plants11141864>>

HAZEN, S. P.; WU, Y.; KREPS, J. A. Gene expression profiling of plant responses to abiotic stress. **Functional & Integrative Genomics**, v. 3, n. 3, p. 105–111, 1 jul. 2003. Available at: <<https://doi.org/10.1007/s10142-003-0088-4>>

HE, Z. et al. The Maize Clade A PP2C phosphatases play critical roles in multiple abiotic stress responses. **International Journal of Molecular Sciences**, v. 20, n. 14, p. 3573, 22 jul. 2019. Available at: <<https://doi.org/10.3390/ijms20143573>>

IPCC. **AR6 Synthesis Report: Climate Change 2022** — IPCC. Available at: <https://www.ipcc.ch/report/sixth-assessment-report-cycle/>.

JIA, F. et al. SCF E3 ligase PP2-B11 plays a positive role in response to salt stress in *Arabidopsis*. **Journal of Experimental Botany**, v. 66, n. 15, p. 4683–4697, 2 jun. 2015a. Available at: <https://doi.org/10.1093/jxb/erv245>

JIA, Y. et al. New insights into the evolutionary history of plant sorbitol dehydrogenase. **BMC Plant Biology**, v. 15, n. 1, 12 apr. 2015b. Available at: <https://doi.org/10.1186/s12870-015-0478-5>

KOLDE, R. **pheatmap: Pretty Heatmaps**. Disponível em: <https://cran.r-project.org/package=pheatmap>.

LI, Q. et al. The *EIL* transcription factor family in soybean: Genome-wide identification, expression profiling and genetic diversity analysis. **FEBS Open Bio**, v. 9, n. 4, p. 629–642, 21 feb. 2019. Available at: <https://doi.org/10.3390/genes11080881>

LI, Y. et al. Transcriptomic analysis revealed the common and divergent responses of maize seedling leaves to cold and heat stresses. **Genes**, v. 11, n. 8, p. 881, 3 aug. 2020. Available at: <https://doi.org/10.3390/genes11080881>

LIU, D. et al. Transcriptome analysis and mining of genes related to shade tolerance in foxtail millet (*Setaria italica* (L.) P. Beauv.). **Royal Society Open Science**, v. 9, n. 10, 1 oct. 2022. <https://doi.org/10.1098/rsos.220953>

LOHSE, M. et al. Mercator: a fast and simple web server for genome scale functional annotation of plant sequence data. **Plant, Cell & Environment**, v. 37, n. 5, p. 1250–1258, 17 dec. 2013. Available at: <https://doi.org/10.1111/pce.12231>

LONI, F. et al. The genomic regions and candidate genes associated with drought tolerance and yield-related traits in foxtail millet: an integrative meta-analysis approach. **Plant Growth Regulation**, 15 may 2023. Available at: <https://link.springer.com/article/10.1007/s10725-023-01010-3>

MA, L. et al. Overexpression of an alfalfa GDP-mannose 3, 5-epimerase gene enhances acid, drought and salt tolerance in transgenic *Arabidopsis* by increasing ascorbate accumulation. **Biotechnology Letters**, v. 36, n. 11, p. 2331–2341, 30 jun. 2014. Available at: <https://doi.org/10.3389/fpls.2020.591911>

MARGIS, R. et al. Glutathione peroxidase family - an evolutionary overview. **FEBS Journal**, v. 275, n. 15, p. 3959–3970, 4 jul. 2008. Available at: <https://doi.org/10.1111/j.1742-4658.2008.06542.x>

MENZ, J. et al. Genome edited crops touch the market: a view on the global development and regulatory environment. **Frontiers in Plant Science**, v. 11, 9 oct. 2020. Available at: <https://doi.org/10.3389/fpls.2020.586027>

MILLER, G. et al. Reactive oxygen species homeostasis and signaling during drought and salinity stresses. **Plant, Cell & Environment**, v. 33, n. 4, p. 453–467, apr. 2010. Available at: <<https://doi.org/10.1111/j.1365-3040.2009.02041.x>>

MITTLER, R. et al. Reactive oxygen gene network of plants. **Trends in Plant Science**, v. 9, n. 10, p. 490–498, oct. 2004. Available at: <<https://doi.org/10.1016/j.tplants.2004.08.009>>

MUHAMMAD, I. et al. Mechanisms regulating the dynamics of photosynthesis under abiotic stresses. **Frontiers in Plant Science**, v. 11, 28 jan. 2021. Available at: <<https://doi.org/10.3389/fpls.2020.615942>>

MURTAGH, F.; LEGENDRE, P. Ward's hierarchical agglomerative clustering method: which algorithms implement ward's criterion? **Journal of Classification**, v. 31, n. 3, p. 274–295, oct. 2014. Available at: <<https://doi.org/10.1007/s00357-014-9161-z>>

MYERS, Z. A. et al. Conserved and variable heat stress responses of the Heat Shock Factor transcription factor family in maize and *Setaria viridis*. **Plant direct**, v. 7, n. 4, 1 apr. 2023. Available at: <<https://doi.org/10.1002/pld3.489>>

NAGARAJU, M. et al. Genome-scale identification, classification, and tissue specific expression analysis of late embryogenesis abundant (*LEA*) genes under abiotic stress conditions in Sorghum bicolor L. **PLOS ONE**, v. 14, n. 1, p. e0209980, 16 jan. 2019. Available at: <<https://doi.org/10.1371/journal.pone.0209980>>

NOCTOR, G.; MHAMDI, A.; FOYER, C. H. The roles of reactive oxygen metabolism in drought: not so cut and dried. **Plant Physiology**, v. 164, n. 4, p. 1636–1648, 7 mar. 2014. Available at: <<https://doi.org/10.1104/pp.113.233478>>

NOURI, M.-Z.; MOUMENI, A.; KOMATSU, S. Abiotic stresses: insight into gene regulation and protein expression in photosynthetic pathways of plants. **International Journal of Molecular Sciences**, v. 16, n. 9, p. 20392–20416, 28 aug. 2015. Available at: <<https://doi.org/10.3390/ijms160920392>>

OSBORNE, C. P.; FRECKLETON, R. P. Ecological selection pressures for C4 photosynthesis in the grasses. **Proceedings of the Royal Society B: Biological Sciences**, v. 276, n. 1663, p. 1753–1760, 25 feb. 2009. Available at: <<https://doi.org/10.1098/rspb.2008.1762>>

PAN, J. et al. Integrative analyses of transcriptomics and metabolomics upon seed germination of foxtail millet in response to salinity. **Sci Rep** v. 10, n. 1, 12 aug. 2020. Available at: <<https://doi.org/10.1038/s41598-020-70520-1>>

PARDO, J.; VANBUREN, R. Evolutionary innovations driving abiotic stress tolerance in C4 grasses and cereals. **The Plant Cell**, v. 33, n. 11, p. 3391–3401, 13 aug. 2021. Available at: <<https://doi.org/10.1093/plcell/koab205>>

QI, X. et al. Genome-wide annotation of genes and noncoding RNAs of foxtail millet in response to simulated drought stress by deep sequencing. **Plant Mol Biol** v. 83, n. 4-5, p. 459–473, 17 jul. 2013. <<https://link.springer.com/article/10.1007/s11103-013-0104-6>>

QIN, L. et al. Genome-wide gene expression profiles analysis reveal novel insights into drought stress in Foxtail Millet (*Setaria italica* L.). **International Journal of Molecular Sciences**, v. 21, n. 22, p. 8520, 12 nov. 2020. Available at: <<https://doi.org/10.3390/ijms21228520>>

R CORE TEAM. **R: The R Project for Statistical Computing**. Available at: <<https://www.r-project.org/>>.

RAMASAMY, A. et al. Key issues in conducting a meta-analysis of gene expression microarray datasets. **PLoS Medicine**, v. 5, n. 9, p. e184, 2 sep. 2008. Available at: <<https://doi.org/10.1371/journal.pmed.0050184>>

RAY, D. K. et al. Recent patterns of crop yield growth and stagnation. **Nature Communications**, v. 3, n. 1, jan. 2012. Available at: <<https://doi.org/10.1038/ncomms2296>>

RAY, D. K. et al. Climate change has likely already affected global food production. **PLOS ONE**, v. 14, n. 5, p. e0217148, 31 may 2019. Available at: <<https://doi.org/10.1371/journal.pone.0217148>>

SAIDI, M. N.; MAHJOUBI, H.; YACOUBI, I. Transcriptome meta-analysis of abiotic stresses-responsive genes and identification of candidate transcription factors for broad stress tolerance in wheat. **Protoplasma**, 5 sep. 2022. Available at: <<https://doi.org/10.1007/s00709-022-01807-5>>

SAURABH KUMAR PANDEY et al. Abiotic stress tolerance in plants: myriad roles of ascorbate peroxidase. **Frontiers in Plant Science**, v. 8, 20 apr. 2017. Available at: <<https://doi.org/10.3389/fpls.2017.00581>>

SHANNON, P. Cytoscape: A software environment for integrated models of biomolecular interaction networks. **Genome Research**, v. 13, n. 11, p. 2498–2504, 1 nov. 2003. Available at: <<https://pubmed.ncbi.nlm.nih.gov/14597658/>>

SHI, W. et al. Transcriptomic studies reveal a key metabolic pathway contributing to a well-maintained photosynthetic system under drought stress in foxtail millet (*Setaria italica* L.). **PeerJ**, v. 6, p. e4752–e4752, 8 may 2018. Available at: <<https://doi.org/10.7717/peerj.4752>>

SHIGEOKA, S. Regulation and function of ascorbate peroxidase isoenzymes. **Journal of Experimental Botany**, v. 53, n. 372, p. 1305–1319, 15 may 2002. Available at: <<https://doi.org/10.1093/jexbot/53.372.1305>>

SUGUIYAMA, V. F., et al. Regulatory mechanisms behind the phenotypic plasticity associated with *Setaria italica* water deficit tolerance. **Plant Molecular Biology**, v. 109, n. 6, p. 761–780, 7 may 2022. Available at: <<https://link.springer.com/article/10.1007/s11103-022-01273-w>>

SUN, L. et al. Integration of metabolomics and transcriptomics for investigating the tolerance of Foxtail Millet (*Setaria italica*) to atrazine stress. **Frontiers in Plant Science**, v. 13, 10 jun. 2022a. Available at: <<https://doi.org/10.3389/fpls.2022.890550>>

SUN, S. et al. Transcriptomic analysis reveals the correlation between end-of-day far red light and chilling stress in *Setaria viridis*. **Genes**, v. 13, n. 9, p. 1565–1565, 31 aug. 2022b. Available at: <<https://doi.org/10.3390/genes13091565>>

SUPIT, I. et al. Assessing climate change effects on European crop yields using the Crop Growth Monitoring System and a weather generator. **Agricultural and Forest Meteorology**, v. 164, p. 96–111, oct. 2012. Available at: <<https://doi.org/10.1016/j.agrformet.2012.05.005>>

TANG, S. et al. Genotype-specific physiological and transcriptomic responses to drought stress in *Setaria italica* (an emerging model for Panicoideae grasses). **Scientific Reports**, v. 7, n. 1, 30 aug. 2017. Available at: <<https://doi.org/10.1038/s41598-017-08854-6>>

THIMM, O. et al. Mapman: a user-driven tool to display genomics data sets onto diagrams of metabolic pathways and other biological processes. **The Plant Journal**, v. 37, n. 6, p. 914–939, mar. 2004. Available at: <<https://doi.org/10.1111/j.1365-313x.2004.02016.x>>

UNITED NATIONS. **World population prospects - population division - united nations**. Available at: <<https://population.un.org/wpp/>>.

USADEL, B. et al. Co-expression tools for plant biology: opportunities for hypothesis generation and caveats. **Plant, Cell & Environment**, v. 32, n. 12, p. 1633–1651, 1 dec. 2009. Available at: <<https://doi.org/10.1111/j.1365-3040.2009.02040.x>>

VAN DIJK, M. et al. A meta-analysis of projected global food demand and population at risk of hunger for the period 2010–2050. **Nature Food**, v. 2, n. 7, p. 494–501, jul. 2021. Available at: <<https://doi.org/10.1093/aob/mcn125>>

VELEY, K. M. et al. *Arabidopsis* MSL10 has a regulated cell death signaling activity that is separable from its mechanosensitive ion channel activity. **The Plant Cell**, v. 26, n. 7, p. 3115–3131, 1 jul. 2014. Available at: <<https://doi.org/10.1105/tpc.114.128082>>

VERGATA, C. et al. Meta-analysis of transcriptomic responses to cold stress in plants. **Functional Plant Biology**, v. 49, n. 8, p. 704–724, 5 apr. 2022. Available at: <<https://doi.org/10.1071/FP21230>>

VERMA, S.; NIZAM, S.; VERMA, P. K. Biotic and abiotic stress signaling in plants. **Stress Signaling in Plants: Genomics and Proteomics Perspective, Volume 1**, p. 25–49, 2013. Available at: <[https://doi.org/10.1007/978-1-4614-6372-6\\_2](https://doi.org/10.1007/978-1-4614-6372-6_2)>

WANG, S. et al. Roles of E3 ubiquitin ligases in plant responses to abiotic stresses. **International Journal of Molecular Sciences**, v. 23, n. 4, p. 2308–2308, 19 feb. 2022. Available at: <<https://doi.org/10.3390/ijms23042308>>

XU, J. et al. Identification and alternative splicing profile of the raffinose synthase gene in grass species. **International Journal of Molecular Sciences**, v. 24, n. 13, p. 11120–11120, 5 jul. 2023. Available at: <<https://doi.org/10.3390/ijms241311120>>



YU, A. et al. Transcriptome and metabolite analysis reveal the drought tolerance of foxtail millet significantly correlated with phenylpropanoids-related pathways during germination process under PEG stress. **BMC Plant Biology**, v. 20, n. 1, 15 jun. 2020. Available at: <<https://doi.org/10.1186/s12870-020-02483-4>>

ZADOKS, J. C.; CHANG, T. T.; KONZAK, C. F. A decimal code for the growth stages of cereals. **Weed Research**, v. 14, n. 6, p. 415–421, dec. 1974. Available at: <<https://doi.org/10.1111/j.1365-3180.1974.tb01084.x>>

ZHANG, G.-B.; MENG, S.; GONG, J.-M. The expected and unexpected roles of nitrate transporters in plant abiotic stress resistance and their regulation. **International Journal of Molecular Sciences**, v. 19, n. 11, p. 3535, 9 nov. 2018. Available at: <<https://doi.org/10.3390/ijms19113535>>

ZHANG, H. et al. Abiotic stress responses in plants. **Nature Reviews Genetics**, p. 1–16, 24 sep. 2021. Available at: <<https://doi.org/10.1038/s41576-021-00413-0>>

ZHANG, L.; ZHANG, X.; FAN, S. Meta-analysis of salt-related gene expression profiles identifies common signatures of salt stress responses in Arabidopsis. **Plant Systematics and Evolution**, v. 303, n. 6, p. 757–774, 10 apr. 2017. Available at: <<https://doi.org/10.1007/s00606-017-1407-x>>

ZHANG, R. et al. Response of multiple tissues to drought revealed by a weighted gene co-expression network analysis in Foxtail Millet [*Setaria italica* (L.) P. Beauv.]. **Frontiers in Plant Science**, v. 12, 12 jan. 2022. <<https://doi.org/10.3389/fpls.2021.746166>>

ZHAO, C. et al. Temperature increase reduces global yields of major crops in four independent estimates. **Proceedings of the National Academy of Sciences**, v. 114, n. 35, p. 9326–9331, 15 aug. 2017. <https://doi.org/10.1073/pnas.1701762114>

## Appendix A - Articles Used In The Meta-Analysis

**Table 2.** Papers analyzed in this study.

Number	Reference
1	ANDERSON, C. M. et al. High light and temperature reduce photosynthetic efficiency through different mechanisms in the C4 model <i>Setaria viridis</i> . <b>Communications Biology</b> , v. 4, n. 1, 16 sep. 2021.
2	DA, Z. et al. Transcriptome analysis reveals key genes in response to salinity stress during seed germination in <i>Setaria italica</i> . <b>Environmental and Experimental Botany</b> , v. 191, p. 104604–104604, 1 nov. 2021
3	GUO, Y. et al. Comparative transcriptomics reveals key genes contributing to the differences in drought tolerance among three cultivars of foxtail millet ( <i>Setaria italica</i> ). <b>Plant Growth Regulation</b> , v. 99, n. 1, p. 45–64, 19 jul. 2022
4	HAN, F. et al. Transcriptome analysis reveals molecular mechanisms under salt stress in leaves of Foxtail Millet ( <i>Setaria italica</i> L.). <b>Plants</b> , v. 11, n. 14, p. 1864–1864, 18 jul. 2022.
5	PAN, J. et al. Integrative analyses of transcriptomics and metabolomics upon seed germination of foxtail millet in response to salinity. <b>Scientific Reports</b> v. 10, n. 1, 12 aug. 2020
6	QI, X. et al. Genome-wide annotation of genes and noncoding RNAs of foxtail millet in response to simulated drought stress by deep sequencing. <b>Plant Molecular Biology</b> v. 83, n. 4-5, p. 459–473, 17 jul. 2013
7	QIN, L. et al. Genome-wide gene expression profiles analysis reveal novel insights into drought stress in Foxtail Millet ( <i>Setaria italica</i> L.). <b>International Journal of Molecular Sciences</b> , v. 21, n. 22, p. 8520, 12 nov. 2020.
8	SHI, W. et al. Transcriptomic studies reveal a key metabolic pathway contributing to a well-maintained photosynthetic system under drought stress in foxtail millet ( <i>Setaria italica</i> L.). <b>PeerJ</b> , v. 6, p. e4752–e4752, 8 may 2018.
9	SUN, S. et al. Transcriptomic analysis reveals the correlation between end-of-day far red light and chilling stress in <i>Setaria viridis</i> . <b>Genes</b> , v. 13, n. 9, p. 1565–1565, 31 aug. 2022b
10	SUGUIYAMA, V. F., et al. Regulatory mechanisms behind the phenotypic plasticity associated with <i>Setaria italica</i> water deficit tolerance. <b>Plant Molecular Biology</b> , v. 109, n. 6, p. 761–780, 7 may 2022

- 11 TANG, S. et al. Genotype-specific physiological and transcriptomic responses to drought stress in *Setaria italica* (an emerging model for Panicoideae grasses). **Scientific Reports**, v. 7, n. 1, 30 aug. 2017.
- 12 YU, A. et al. Transcriptome and metabolite analysis reveal the drought tolerance of foxtail millet significantly correlated with phenylpropanoids-related pathways during germination process under PEG stress. **BMC Plant Biology**, v. 20, n. 1, 15 jun. 2020.
- 13 ZHANG, R. et al. Response of multiple tissues to drought revealed by a weighted gene co-expression network analysis in Foxtail Millet [*Setaria italica* (L.) P. Beauv.]. **Frontiers in Plant Science**, v. 12, 12 jan. 2022
-

## Appendix B - Metadata

**Table 3.** Detailed information about comparisons.

<b>Comparison ID</b>	<b>Species</b>	<b>Stress Type</b>	<b>Tissue</b>	<b>Days</b>	<b>Stage</b>	<b>Reference Number</b>
Si02Se	<i>Setaria italica</i>	Salt	Seeds	3	germination	2
Si03Se	<i>Setaria italica</i>	Salt	Seeds	3	germination	2
Si04Se	<i>Setaria italica</i>	Salt	Seeds	7	germination	2
Si05Se	<i>Setaria italica</i>	Salt	Seeds	7	germination	2
Si06Sr	<i>Setaria italica</i>	Salt	Roots	7	germination	5
Si07Sr	<i>Setaria italica</i>	Salt	Roots	7	germination	5
Si08Sr	<i>Setaria italica</i>	Salt	Roots	7	germination	5
Si09Sr	<i>Setaria italica</i>	Salt	Roots	7	germination	5
Si10Ss	<i>Setaria italica</i>	Salt	Shoots	6	germination	4
Si11Ss	<i>Setaria italica</i>	Salt	Shoots	6	germination	4
Si12Ds	<i>Setaria italica</i>	Drought	Shoots	34	seedling	8
Si13Dr	<i>Setaria italica</i>	Drought	Roots	34	seedling	8
Si14Ds	<i>Setaria italica</i>	Drought	Shoots	59	jointing	13
Si15Ds	<i>Setaria italica</i>	Drought	Shoots	59	jointing	13
Si16Dr	<i>Setaria italica</i>	Drought	Roots	59	jointing	13
Si17Ds	<i>Setaria italica</i>	Drought	Shoots	59	jointing	13
Si18Ds	<i>Setaria italica</i>	Drought	Shoots	59	jointing	13
Si19Dr	<i>Setaria italica</i>	Drought	Roots	59	jointing	13
Si20Ds	<i>Setaria italica</i>	Drought	Shoots	59	jointing	13
Si21Ds	<i>Setaria italica</i>	Drought	Shoots	59	jointing	13
Si22Dr	<i>Setaria italica</i>	Drought	Roots	59	jointing	13
Si23Ds	<i>Setaria italica</i>	Drought	Shoots	59	jointing	13
Si24Ds	<i>Setaria italica</i>	Drought	Shoots	59	jointing	13
Si25Ds	<i>Setaria italica</i>	Drought	Shoots	32	seedling	3

Si26Ds	<i>Setaria italica</i>	Drought	Shoots	32	seedling	3
Si27Ds	<i>Setaria italica</i>	Drought	Shoots	32	seedling	3
Si28Ds	<i>Setaria italica</i>	Drought	Shoots	31	seedling	11
Si29Ds	<i>Setaria italica</i>	Drought	Shoots	31	seedling	11
Si30Ds	<i>Setaria italica</i>	Drought	Shoots	31	seedling	11
Si31Ds	<i>Setaria italica</i>	Drought	Shoots	52	jointing	10
Si32Ds	<i>Setaria italica</i>	Drought	Shoots	52	jointing	10
Si33Ds	<i>Setaria italica</i>	Drought	Shoots	23	seedling	7
Si34Ds	<i>Setaria italica</i>	Drought	Shoots	23	seedling	7
Si35Dr	<i>Setaria italica</i>	Drought	Roots	23	seedling	7
Si36Dr	<i>Setaria italica</i>	Drought	Roots	23	seedling	7
Si37Ps	<i>Setaria italica</i>	PEG	Shoots	14	seedling	6
Si38Pe	<i>Setaria italica</i>	PEG	Seeds	7	germination	12
Sv41Ls	<i>Setaria viridis</i>	High light	Shoots	14	seedling	1
Sv42Ls	<i>Setaria viridis</i>	High light	Shoots	14	seedling	1
Sv43Ls	<i>Setaria viridis</i>	High light	Shoots	14	seedling	1
Sv44Hs	<i>Setaria viridis</i>	Heat	Shoots	14	seedling	1
Sv45Hs	<i>Setaria viridis</i>	Heat	Shoots	14	seedling	1
Sv46Hs	<i>Setaria viridis</i>	Heat	Shoots	14	seedling	1
Sv47Cs	<i>Setaria viridis</i>	Cold	Shoots	23	seedling	9
Sv48Cs	<i>Setaria viridis</i>	Cold	Shoots	23	seedling	9
Sv49Cs	<i>Setaria viridis</i>	Cold	Shoots	23	seedling	9
Sv50Cs	<i>Setaria viridis</i>	Cold	Shoots	23	seedling	9
Sv51Cs	<i>Setaria viridis</i>	Cold	Shoots	23	seedling	9
Sv52Cs	<i>Setaria viridis</i>	Cold	Shoots	23	seedling	9

---